www.mycoordinates.org

Coordinates

Volume XIII, Issue 12, December 2017

THE MONTHLY MAGAZINE ON POSITIONING, NAVIGATION AND BEYOND

Crowd monitoring
through WiFi data

POSITIONING • GNSS • NAVIGATION

Leica Pegasus:Two
Mobile reality capture

Leica Pegasus:Two creates new business opportunities by leveraging the concept of a multisensor platform, enabling you to add pavement assessment cameras and sky cameras for city modelling, ground penetrating radar or thermal imaging, noise pollution, and air quality sensors. By moving the work from the field to the office, employees are safer, insurance is less, deployment is faster, and site visits are decreased.

Vehicle and application independent

Visit **www.leica-geosystems.com** Mobile Sensor Platforms for more information or to request a demo.

Leica Geosystems AG
www.leica-geosystems.com

- when it has to be **right**

LabSat3 WIDEBAND

The most powerful LabSat yet, the new LabSat 3 WIDEBAND captures and replays more GNSS signals at a much higher resolution than before.

Small, battery powered and with a removable solid state disk, **LabSat 3 WIDEBAND** allows you to quickly gather detailed, real world satellite data and replay these signals on your bench.

With three channels, a bandwidth of up to 56MHz and 6 bit sampling, **LabSat 3 WIDEBAND** can handle almost any combination of constellation and signal that exists today, with plenty of spare capacity for future planned signals.

LabSat 3 WIDEBAND can record and replay the following signals:

- GPS: L1 / L2 / L5
- GLONASS: L1 / L2 / L3
- BeiDou: B1 / B2 / B3
- QZSS: L1 / L2 / L5
- Galileo: E1 / E1a / E5a / E5b / E6
- SBAS: WAAS, EGNOS , GAGAN, MSAS, SDCM
- IRNSS

www.labsat.co.uk

In this issue

Coordinates Volume 13, Issue 12, December 2017

Articles

Columns

Collapse of Global village?

It was about globalization.

Open economy, free trades, …

Political barriers were overtaken by economic interests.

The world saw a common interest in working together.

A successful example of that is European Union.

However, a perception is gathering momentum

That some gained more at the expense of others.

Hence, the trend is reversing.

It is again becoming about

Our people, our country…

Protectionism is knocking at the door

Of the global village,

It may even knock-it-out.

Wishing all esteemed readers of Coordinates

A healthy and happy year 2018.

Bal Krishna, Editor
bal@mycoordinates.org

The generation of well geo-referenced floor plans in indoor navigation system

This study concentrates on generating the highly accurate floor plans based on the robot mapping technique using the portable mapping system

Guang-Je Tsai
Department of Geomatics Engineering, National Cheng-Kung University, Taiwan

Kai-Wei Chiang
Department of Geomatics Engineering, National Cheng-Kung University, Taiwan
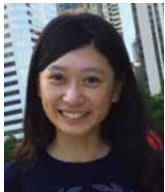
Min-Chuan Tsai
Department of Geomatics Engineering, National Cheng-Kung University, Taiwan

You-Liang Chen
Department of Geomatics Engineering, National Cheng-Kung University, Taiwan
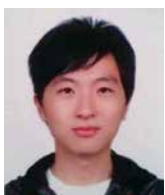
Jhen-Kai Liao
Department of Geomatics Engineering, National Cheng-Kung University, Taiwan

In the past few years, Mobile Mapping System (MMS) has been widely used in Geomatics engineering. Using various mapping sensors, such as Light Detection And Ranging (LiDAR), camera and high resolution visible sensors, geospatial information can be easily acquired by a mobile platform. The most common mobile mapping systems work by capturing more than one image which include the same feature point, captured from different perspective, allowing the 3D spatial information of objects to be calculated and measured with respect to the mapping frame (Tao et al. 2001). MMS is also being used with various vehicles, such as automobiles, aircraft, water-based vessels and Unmanned Aerial Vehicles (UAV). More recently, the use of MMS has not been restricted to being mounted on mobile machines. A portable MMS has been proposed which is composed of a Position and Orientation System (POS) module working in conjunction with an image acquisition module, trigger control and data logging module (Chu et al. 2013). This system could be used in some areas that are inaccessible to vehicles.

Because of the increasing demand for accurate indoor maps, MMS has evolved to the next phase: indoor environment. This application would be useful for emergency, indoor navigation, as well as Location-Based Services (LBS), etc. In fact, high accuracy map of indoor environments, once it caught on, would soon become indispensable in indoor navigation and LBS. In general, building blueprints are not easy to access; determining and

evaluating the absolute accuracy of these blueprints are a logistical nightmare. In robotics research, most robotic navigation tasks are based on the building maps, therefore, methods for generating relatively reliable floor plans has become an important topic (Okorn et al. 2010). Robot mapping systems focus on real time localization, sensing and measuring the environment at the same time; as a result, Simultaneously Localization and Mapping (SLAM) algorithms are widely used in robot applications.

After analyzing previous researches, most robot mapping systems concentrate on developing high efficient SLAM algorithms or using different platforms to implement the SLAM. However, these floor plans generated by the robot mapping are limited to certain mapping system and therefore, lack of generalization. Even though the maps are produced by the same system, it requires extra works to relocate the position and reorientation manually in order to reuse the produced maps. Besides, floor plans generated by the SLAM are hard to evaluate the accuracy and can't directly be used in other applications. The main problem is that these floor plans are not in the standard coordinate frame and therefore it is tough to use. This study proposes the modules for generating indoor floor plan that can transfer the local map reference in robot system into well geo-referenced map. This kind of map can be applied for various seamless applications, such as the navigation system from outdoor to indoor. Also, this study uses the sketch

maps of building to create the indoor floors map compared with the maps by SLAM. To evaluate the absolute positioning accuracy and rectify the indoor floor plans from different platforms, this study built the testing and calibration field based on the control survey to analyze each result for purposes of cross validation.
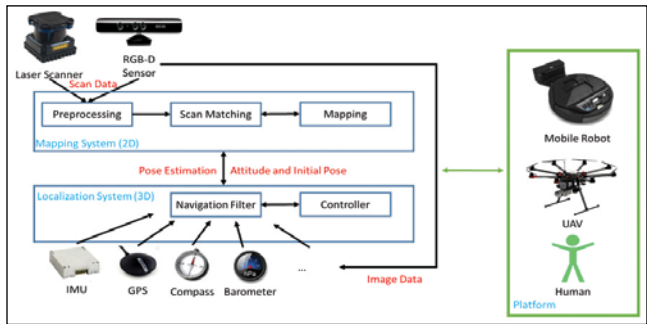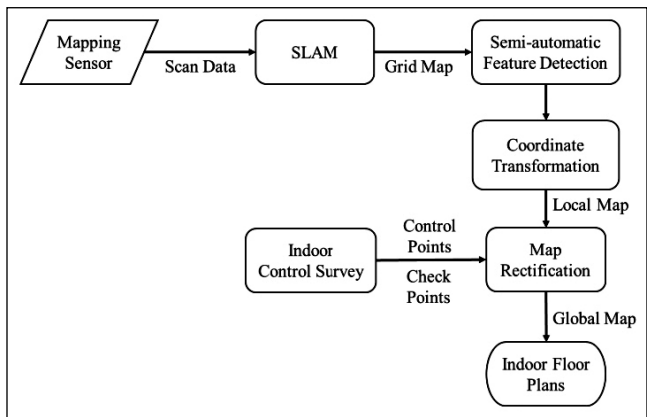

Figure 1: Indoor MMS payload design

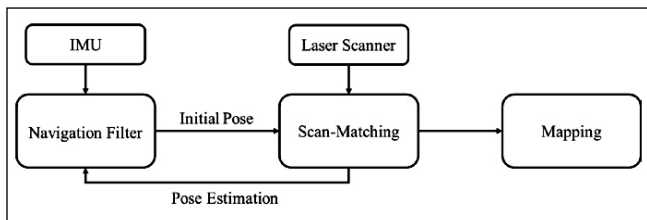**Figure 2: The flow chart of floor plans generalization**

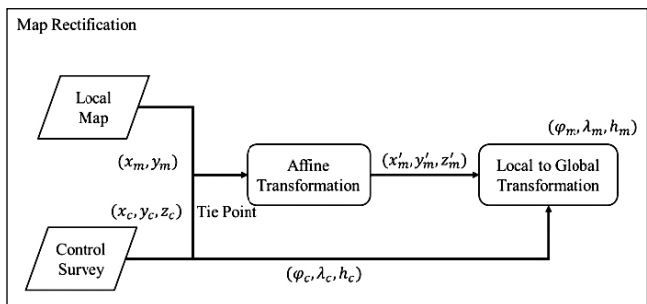**Figure 3: The data process of Hector SLAM**

Figure 4: The flow chart of map rectification

Indoor MMS design and implementation

To implement the indoor MMS, the payload design of this study is divided into two parts, namely localization and mapping. In the localization system, GPS/INS (Inertial Navigation System) is the primary integration system that generates the global position information for the mapping system and enables the user to move seamlessly from outdoor to indoor environments (and vice versa) based on the produced floor plans with a global coordinate system. In the design of this localization system, aiding information, such as heading data from a digital compass, height difference calculated based on atmospheric pressure, and even the velocity and attitude states determined from sequential images, is used to update the navigation filter as well. The mapping system, which includes a laser scanner and an RGB-D sensor, is used to derive the scan data. It is important for the mapping system to conduct preprocessing and calibration before the mapping process to improve accuracy. The data from each scan is combined with position and attitude information in order to register the different datasets together with the position and attitude feedback to the navigation filter. This common payload is designed not only for robots and UAVs, but also for human carriers and other mobile platforms. The payload design is presented in Figure 1.

Methodology

SLAM has been developed for many years, and most algorithms achieve the robust performance on mapping system as well as localization. The generated map often used in navigating the robot and implementing the autonomous motion planning. In this study, the issued problem is that if user wants to update the map or implement the motion planning with known map, it needs to take extra efforts to initialize the position and orientation. It is also known as global localization problem that puts the robot into the known environment and has to localize itself from scratch. The primary issue is that the map is often generated in different reference frames. This problem also occurs when users apply the robot map on different applications. Another problem is that without any landmarks or absolutely aiding information, the accuracy of robot mapping is degraded with time. Therefore, this study proposes the novel map rectification process to rectify and transfer the raw map into the global frame with reliable scale and accuracy. Figure 2 shows the floor plan generalization processes and the detail is described below.

Hector SLAM

SLAM is a common solution that senses and recreates the map of an unknown environment and simultaneously tracks the position and attitude of the platform in robot research. The core integrating algorithms are classified into three paradigms, Kalman filters, particle filters and graph-based processing. In SLAM applications, most of algorithms rely on environmental landmarks and the sensors' raw-data which are integrated into the SLAM model. For the robot map, occupancy grid maps cut the environment

into the small cells, each of which includes different attributes to represent the environment. An occupancy grid maps record the whole environment information that sensors observe and transfer it into the occupancy grid. This study aims at using grid-based SLAM algorithms, Hector SLAM, to generate the floor plans.

Due to the rapid development of mapping and localization sensors, most robots are equipped with a payload of a small laser scanner and MEMS IMU. Hector SLAM is one of the SLAM algorithms developed for laser scanners (Kohlbrecher, 2011). The main differences between these two SLAM algorithms are the 6 DOF motion estimation without odometry and scan-matching method. Figure 3 shows a flow chart of Hector SLAM process. This means the mapping system doesn't have to be mounted on at mobile robot; it could be mounted on UAV, human or other platforms without odometer.

The estimated pose information is an important parameter for scan-matching; it improves the performance. In addition, scan-matching also gives the posterior information to enhance the navigation results. Scan-matching plays a significant role in Hector SLAM. In the process, the data from the laser scanner is aligned with the map or other observations. Based on the high accuracy of laser scanners, with low distance measurement noise and high scan rates, scan-matching provides 2D pose estimation for the navigation filter by registering each piece of scanned data and aligning it with the existing map. This approach is based on the optimization of aligning the endpoint of the scan data and the existing map. The basic idea is follows the Gauss-Newton approach from (Lucas et al., 1981).

Map rectification

In order to deal with the scale and deformation problems of generated map from different mapping systems, this study proposes the new method to refine the map and also implements the coordinate transformation to generate the map in global frame. The flow chart is shown in the Figure 4. In the beginning, the local map and control points are located in the same coordinate system. For rectifying the map, map rectification uses the affine transformation that includes 6 parameters, two translations, two scale, rotation and shear. In this transformation, it needs to select at least three tie points from control survey in order to calculate 6 parameters and eliminate the deformation problem. Therefore, there is a significant correlation between tie points selection and the accuracy of rectified map. Tie points should be widely and uniformly placed at distorted area to control deformation. Finally, the rectified map (x'_m, y'_m, z'_m) is transferred into global coordinate $(\varphi_m, \lambda_m, h_m)$ by using the local to global transformation.

Experiment

Because the accuracy of the indoor map is not easy to assess and evaluate, this study adopts an indoor control survey for the mapping experiments. Before conducting the experiments, a control survey was established by using angle and distance

measurements observed by a high accuracy device. A sketch of the control survey is shown in Figure 5; the triangular points represent the control points, and the green points are the check points located in the building's corners for evaluating the floor plan. These check points measured by the control survey are represented as the building's boundary features to compare with floor plan. Total experimental area is about 1300 square meters, the width is about 30 meters and the length is about 60 meters.

In this experiment, we deployed laser scanner (UST-20LX) using handheld approach to analyze and evaluate the performance of indoor floor plans. The configuration shown in Figure 6.

Results and discussions

After the scan of the laser scanner, the raw map of the environments are derived. Since the distroted and the scale problems mentioned above, we continue with the map rectification. Figure 7 and figure 8 show the comparison between generated maps. The triangular points stand for control points, the red points are the check points, and black points are used to do the affine transformation. Others can be the index of the accuracy analysis.
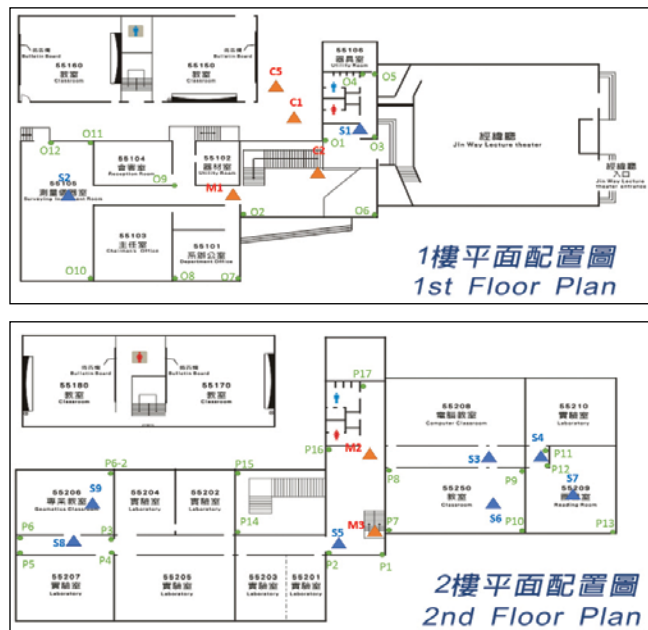

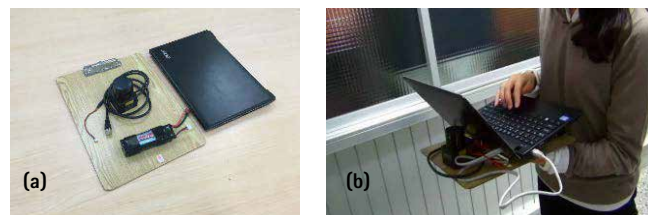Figure 5: The sketch of indoor control points and check points

Figure 6: The indoor MMS using handheld approach, (a) shows payload for handheld approach; (b) shows actual operation for handheld approach

Take a look at relative positions of the points and the maps, as the check points are all designed in the corner, most of the points in laser scanner receiving maps match the corners that they should be. On the other hand, the maps generated by sketch maps have more displacements from the positions that the points belong to. In figure 7, the scale problem is obvious in the right part of both figure. The length of the space is range from 20 m in sketch generated map to 30 m in laser scanner received map. In figure 8(b), there is a trend for the check points and the positions they should locate. All of the should-be corners are in the right of each corresponding check points. It shows the posibility to calibrate this problem with the similar situation. However, the conditions in figure 8(a) are too random that depending on the sketch maps creator. To be more convincing, this paper looks deeply into the values and do some calculations. From the comparisons of figure 7 and figure 8, the coordinates turn out to be the calculations of the points' accuracy. The indexes include average errors, standard deviation and RMSE.

Figure 9 shows the computation in histograms for 1st and 2nd floor respectly. Each histogram has the comparison of generated maps between sketch map method and handheld approach.

We can tell from figure 9 that most of the blue histograms get higher than the gray ones. That is to say, almost all of the computations support laser scanner has better result than the method of sketch map. Besides, the accuracy reaches the goal within 1 meter. Since the outcomes from sketch map has a better results in 2nd floor than in 1st floor. It's assumed that the more check points, the more possible to get greater calculations. As standard deviation results always preferable than RMSE outcomes, the problem to get well geo-referenced floor plans should be considered.

Conclusion

In order to improve the accuracy of the indoor floor plans generated by sketch maps, this study turns to the robot mapping technique with the portable mapping system to produce highly accurate floor plans. Existed sketch maps should be convenient but the accuracy isn't quite suitable for indoor navigation. However, we know that indoor environment is relatively narrow than outdoor environment. Therefore, the accuracy must also be in a rather strict level.

Based on the map rectification approach using the affine transformation, this study solves the scale and deformation problems out of the former method. With the calibration field built by traditional outdoor control survey method, the absolute accuracy of indoor floor plans can be evaluated. At the same time, this study has been able to illustrate the portable robotic mapping system really working out well. Since the average errors, RMSE and standard deviation in this study are all within 1 meter, it goes without saying that the approach certainly meets the usage for indoor navigation maps. When compare with the sketch map method, it also gets better

accuracy. Finally, this study clearly demonstrates that the building floor plans reach 1-meter absolute positioning accuracy by proposed portable mapping systems and rectified sketch maps combined with the map rectification.

Acknowledgement

References

[1]   Tao, V.C.; Li, J. (2001). Advances in mobile mapping technology. International Society for Photogrammetry and Remote Sensing (ISPRS) Book Series: Taylor and Francis Group: London, UK.

[2]   Eisenbeiss, H. (2004). A mini unmanned aerial vehicle (uav): System overview and image acquisition. In: Proceedings of the International Workshop on Processing and Visualization Using HighResolution Imagery, Pitsanulok, Thailand.

[3]   Neitzel, F.; Klonowski, J. (2012). Mobile 3d mapping with a low-cost uav system. In: International Conference on Unmanned Aerial Vehicle in Geomatics (UAV-g), Vol. XXXVIII-1/C22, pp 39-44.

[4]   Chu, C.H.; Chiang, K.W.; Lin, C.A. (2013). The performance analysis of a portable mobile mapping system with different gnss processing strategies, Proceedings of the 26th International Technical Meeting of The Satellite Division of the Institute of Navigation (ION GNSS+ 2013), Nashville, TN, September, pp 689 - 703.

[5]   Okorn, B.; Xiong, X.; Akinci, B.; Huber, D. (2010). Toward automated modeling of floor plans, Proceedings of the Symposium on 3D Data Processing, Visualization and Transmission Paris, France, 5/17.

[6]   Grzonka, S.; Grisetti, G.; Burgard, W. (2009). Towards a navigation system for autonomous indoor flying. In Robotics and Automation. ICRA '09. IEEE International Conference on, IEEE: Kobe; pp 2878 - 2883.

[7]   Fallon, M. F.; Johannsson, H.; Brookshire, J.; Teller, S.; Leonard, J. J. (2012). Sensor Fusion for Flexible Human-Portable Building-Scale Mapping. Intelligent Robots and Systems (IROS), IEEE/RSJ International Conference on, IEEE: Vilamoura, pp 4405-4412.

[8]   Kohlbrecher, S.; von Stryk, O.; Meyer, J.; Klingauf, U. (2011). A flexible and scalable slam system with full 3d motion estimation. In Safety, Security, and Rescue Robotics (SSRR), 2011 IEEE International Symposium on, IEEE: Kyoto; pp 155 – 160.

[9]   Grisetti, G.; Stachniss, C.; Burgard, W. (2007). Improved techniques for grid mapping with rao-blackwellized particle filters. Robotics, IEEE Transactions on 2007, 23, 34 - 46.

[10] Kaplan, E.D. (1996). Understanding gps: Principles and applications. Artech House.

[11] Wolf, P.R.; Ghilani, C.D. (2006). Elementary surveying: An introduction to geomatics. Pearson/Prentice Hall.

[12] Van der Heijden, F. (1995). Edge and line feature extraction based on covariance models. Pattern Analysis and Machine Intelligence, IEEE Transactions on 1995, 17, 16-33.

[13] Chiang, K.W.; Liao, J.K.; Tsai, G.J.; Chang H.W. (2015). The performance analysis of the map-aided fuzzy decision tree based on the pedestrian dead reckoning algorithm in an indoor environment, TN, December.
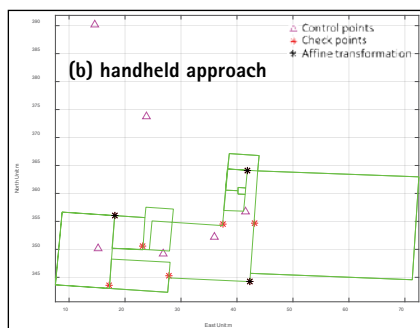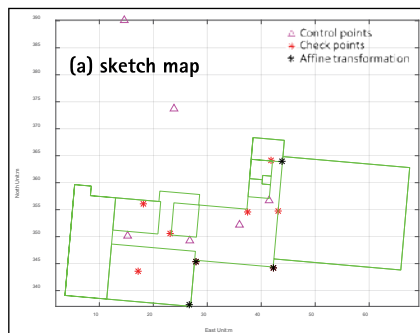
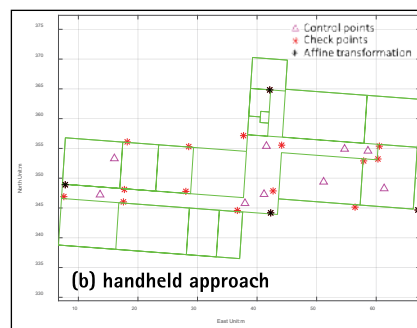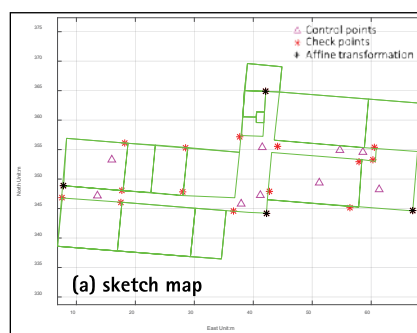Figure 7: The generated map using sketch map and handheld approach (1F)

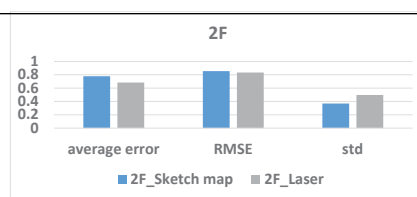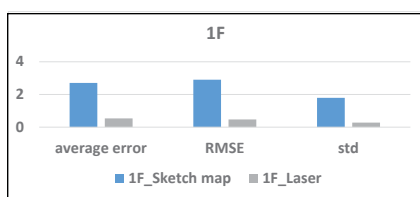Figure 8: The generated map using sketch map and handheld approach (2F)

Figure 9: The statistic of generated map

Performance evaluation of Single Baseline and Network RTK GNSS

The aim of this study is to compare a 'Single Baseline RTK' and a 'Network RTK' approaches with respect to performance and accuracy

Reha Metin ALKAN
Prof. Dr, Hitit University, Çorum, Turkey & Istanbul Technical University, Istanbul, Turkey

İ. Murat OZULU
Lecturer, Hitit University, Çorum, Turkey

Veli İLÇİ
Assist.Prof. Dr, Hitit University, Çorum, Turkey

A couple of decades ago, it was necessary to collect carrier-phase data with at least two GPS receivers simultaneously within a few hours to make high accuracy positioning. Developments in the satellite geodesy and processing technique as well satellite and receiver systems, a method called as Real-Time Kinematic (RTK) Positioning using corrections for rover receiver from a reference station has begun to serve as an accurate and efficient surveying method for different users all over the world since the 1990s. This method also referred as Single Baseline RTK because single baseline solution is used in order to make positioning. On the other hand, the usability of this method is limited with the distance between the user receiver and its base station due to orbital, ionospheric and tropospheric biases that deteriorate the positioning. This also means, usability and performance of Single Baseline RTK method is highly dependent on the distance between rover and its reference station. The quality of the estimated errors degrades as a function of distance between the base station and the rover. In this method distance-dependent biases, such as orbital, ionospheric, and tropospheric biases deteriorate the

positioning accuracy and depending on this, the baseline length is restricted to about 10-20 km (El-Mowafy 2012). When the baseline length increases, the errors at reference and rover receivers become less common and therefore cannot be cancelled out properly. This causes to lower positional accuracy when the longer distance was established during the Single Baseline RTK Positioning.

For the last one or two decades, many governments, municipalities and private sectors have established national and/or international Continuously Operating Reference Stations (CORS) Networks all over the world for many purposes such as geodesy, geophysics, navigation, surveying, precision agriculture, aviation, transportation, etc. For instance, Turkey has approximately 150 reference stations with an average distance of 70-100 km, Germany has approximately 270 reference stations with an average distance of about 40 km, Switzerland has 31 stations with an average distance of 35-50 km, Sweden has 170 stations with an average distance of 60-70 km, Korea has 60 stations with an average distance of 40 km and Indonesia has more than 230 CORS stations (Alkan et al. 2017; Kim et al. 2017).

Table 1. Main advantages and disadvantages of the Network RTK method

Advantages	Disadvantages
- Reducing the surveying time, cost and labour of the field work since there is no need of observations occupied on known points and at least two receivers, - More economical and rapid solutions, - Higher reliability and availability of RTK corrections with improved redundancy, - Homogeneous high accuracy (cm-level) with more flexibility (up to 100 km), - Continuously monitored reference stations and updated coordinates in the event of any deformation, - Positioning without interruption in the case of a reference station being out of order since there is another station immediately to take its place.	- Necessity of subscription at cost, - Dependence on an external source to provide essential information, - Dependence of data communication between the computing centre and the user, - Dependence on coverage of GSM carrier service and being not available at all areas or having temporary interruptions, - Communication cost, - Interruption of the survey due to the probable network breakdowns, - Necessity of more complicated and more expensive geodetic-grade GNSS receiver and equipment with Network RTK capability.

At the beginning of 2000s, multi-baseline RTK positioning, known as Network RTK, has resulted by adding real-time kinematic positioning ability to the established CORS Networks (Wanninger 2006). In this method, GNSS raw data gathered from the CORS Network in order to create models that can mitigate these errors acting within the CORS coverage area (Aponte et al. 2008). The number and extent of governmental and private Network RTKs all over the world have been increasing while reducing the positioning cost. Compared to Single Baseline RTK in Network RTK method, the distance-dependent errors mentioned above are modelled more conveniently especially for long baselines i.e. several tens of kilometres (Ogutcu and Kalayci 2016).

This improves the accuracy and reliability of positioning over extended distances and (Denys and Pearson 2016) this technique provides homogenous accuracy and better positioning. Thus, the most accurate real-time kinematic positioning method is Network RTK that uses corrections from a network of reference stations (Prochniewicz et al 2017). In this method, there are several correction techniques that have been implemented and used like Virtual Reference Station (VRS), Flächen-Korrektur Parameter (FKP), Individualized Master-Auxiliary Corrections (iMAX), Master-Auxiliary Concept (MAC), and Pseudo Reference Station (PRS). Despite of its several important advantages which were mentioned above, this method has also some disadvantages. The main advantages and disadvantages of the Network RTK are summarized in Table 1 (Kahveci 2009; El-Mowafy 2012).

The Network RTK provides more convenient, cost-effective and real-time precise positioning and thus has been extensively used by surveyor. This method makes GNSS a very efficient tool for land, air, marine and numerous different types of applications where precise real-time positioning is required. More information can be found in Fotopoulos and Cannon (2001); Lachapelle and Alves (2002); Rizos (2002); Rizos (2007); El-Mowafy (2012) and Cina et al. (2015).

Many administrative entitles and private organizations have established their own Single Baseline RTK as well as Network RTK in all over the world. One of them was established and operated by Çorum Municipality, Turkey to serve Çorum province. Concerning the Network RTK, there is a network called as TUSAGA-Aktif (CORS-TR) and it has begun to serve for civilian users since 2009. This network has 2 Control and 146 Reference Stations with an average spacing of about 70-100 km as it is covered almost the entirely of Turkey and Turkish Republic of Northern Cyprus. In this system, VRS, FKP and MAC correction techniques are

Table 2. Some technical features of receiver, Trimble R10, used in this study (URL 1). More information about the receivers used in this study can be found in URL 1.

PERFORMANCE SPECIFICATIONS	Measurements
	• Satellite signals tracked simultaneously:
	– GPS: L1C/A, L1C, L2C, L2E, L5
	– GLONASS: L1C/A, L1P, L2C/A, L2P, L3
	– SBAS: L1C/A, L5 (For SBAS satellites that support L5)
	– Galileo: E1, E5a, E5B
	– BeiDou (COMPASS): B1, B2
	• CenterPoint RTX, OmniSTAR HP, XP, G2, VBS positioning
	• QZSS, WAAS, EGNOS, GAGAN
	• Positioning Rates: 1 Hz, 2 Hz, 5 Hz, 10 Hz, and 20 Hz

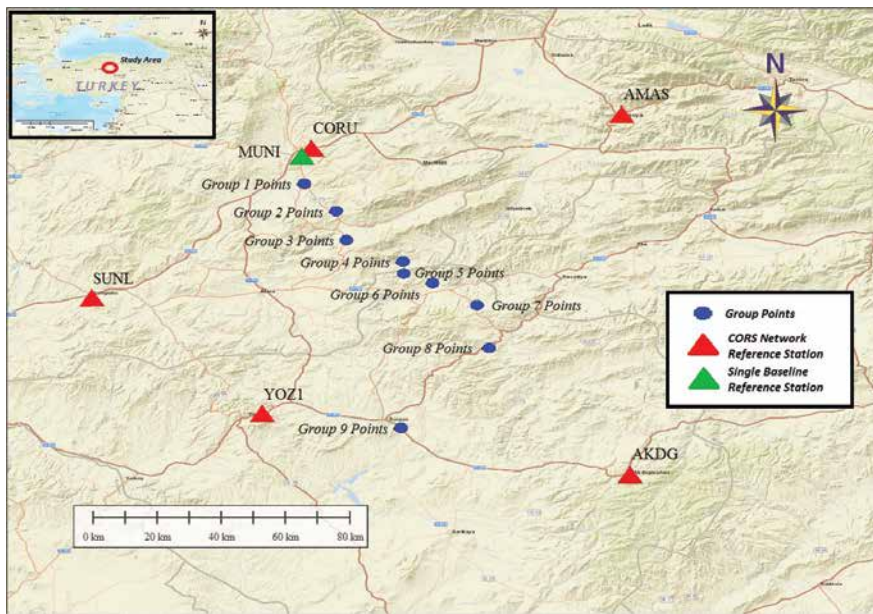| POSITIONING PERFORMANCE		
Static GNSS Surveying		
High-Precision Static		
Horizontal	3 mm + 0.1 ppm RMS	
Vertical	3.5 mm + 0.4 ppm RMS	
Static and Fast Static		
Horizontal	3 mm + 0.5 ppm RMS	
Vertical	5 mm + 0.5 ppm RMS	
Real Time Kinematic Surveying		
Single Baseline < 30 km		
Horizontal	8 mm + 1 ppm RMS	
Vertical	5 mm + 1 ppm RMS	
Network RTK		
Horizontal	8 mm + 0.5 ppm RMS	
Vertical	15 mm + 0.5 ppm RMS	

Figure 1. The location of established points

used. The coordinates can be obtained in ITRF96 datum and 2005.0 measurement epoch. More information about Turkish RTK CORS Network, i.e., TUSAGA-Aktif (CORS-TR) System can be found in Eren et. al. (2009); Mekik et al. (2011); Bakıcı and Mekik (2014) and Bakıcı (2015).

The main objective of this study is to assess accuracy performance of the 'Single Baseline RTK' operated by Çorum *Local Municipality* and the 'Network RTK' operated by *Republic of Turkey, General Directorate of Land Registry and Cadastre*. For this purpose, a number of static experiments were conducted. The test procedures and obtained results with some recommendations are given.

Test measurement

In order to compare and assess the performance of the Single Baseline RTK and Network RTK, test measurements were carried out in City of Çorum district, Turkey on May 2017 (GPS Day of Year 145 and 147). As stated in previous chapter, Single Baseline RTK is affected by the distance dependent errors. In this study, it was also investigated how the accuracy would be affected depending on the distance from the used Single Baseline's base (reference) station. For this purpose, 9 group of points (each group consist of 3 points) were established. The approximate distances from the base station (MUNI) of Single Baseline RTK to established points are:

- 9 km for Group 1 Points,
- 19 km for Group 2 Points,
- 28 km for Group 3 Points,
- 41 km for Group 4 Points,
- 44 km for Group 5 Points,
- 50 km for Group 6 Points,
- 62 km for Group 7 Points,
- 74 km for Group 8 Points,
- 87 km for Group 9 Points.

The location of the established points including reference stations in the vicinity of the measurement area are shown on a map (Figure 1).

As a first step of the test measurements, the coordinates of the newly established points

were determined in real-time with Network RTK approach. The coordinates of the same points were then determined again with Single Baseline RTK after cold-start of the receivers. During the survey, after fixed solutions obtained (mostly within less than 1 minute), 10 observation epochs were collected with1-second measurement interval and the average value of these 10 epochs was recorded as a point's

coordinate. In the test measurements, with VRS correction technique by observing all visible GPS and GLONASS satellites above 10-degree elevation mask.

In order to determine the reference (known) coordinates of these points, static GNSS measurements were carried out about 45 minutes to 1 h occupation time. During the post-processing stage, 5 of the

Table 3. Differences between known and RTK–derived coordinates

| Distance from used single baseline's base station	Point number	Differences (m)			
		for Network RTK		for Single baseline RTK	
		2D Position	Height	2D Position	Height
9 km	R1	0.03	-0.01	0.02	-0.05
	R2	0.06	-0.03	0.05	-0.02
	R3	0.03	-0.02	0.03	-0.01
19 km	R1	0.01	0.00	0.02	-0.01
	R2	0.02	0.00	0.00	0.00
	R3	0.01	0.00	0.02	-0.03
28 km	R1	0.01	-0.03	0.02	-0.05
	R2	0.01	-0.02	0.01	-0.01
	R3	0.01	0.01	0.02	-0.03
41 km	R1	0.02	0.01	0.04	-0.01
	R2	0.03	0.00	0.02	0.02
	R3	0.02	-0.01	0.02	0.00
44 km	R1	0.03	-0.01	0.05	-0.08
	R2	0.03	0.01	0.08	0.08
	R3	0.02	0.03	0.05	0.01
50 km	R1	0.04	0.00	0.05	-0.04
	R2	0.02	-0.05	0.03	-0.06
	R3	0.02	0.00	0.04	-0.02
62 km	R1	0.04	0.01	0.04	-0.02
	R2	0.03	0.00	0.03	-0.06
	R3	0.03	0.01	0.04	-0.02
74 km	R1	0.01	-0.04	0.07	-0.10
	R2	0.04	0.00	0.02	-0.02
	R3	0.04	-0.01	0.02	-0.05
87 km	R1	0.08	0.13	0.06	0.08
	R2	0.03	0.02	0.20	-0.01
	R3	0.04	0.01	0.04	-0.07
Statistics	Min.	0.01	0.00	0.00	0.00
	Max.	0.08	0.13	0.20	0.10
	Mean	0.03	0.02	0.05	0.04
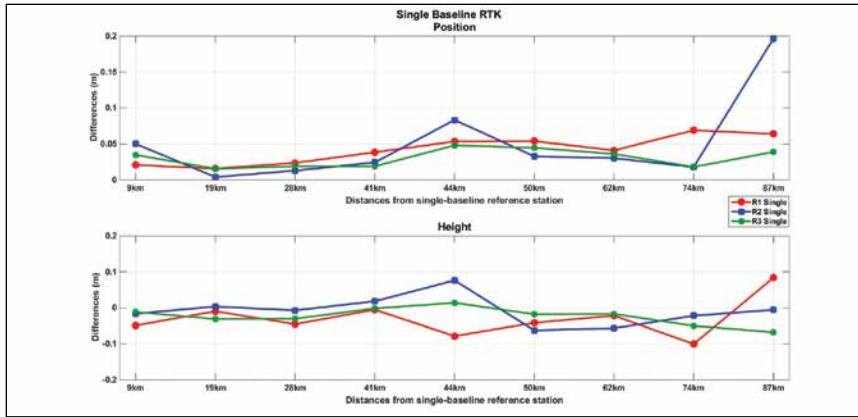
Figure 2. Differences between known and single baseline RTK–derived coordinates
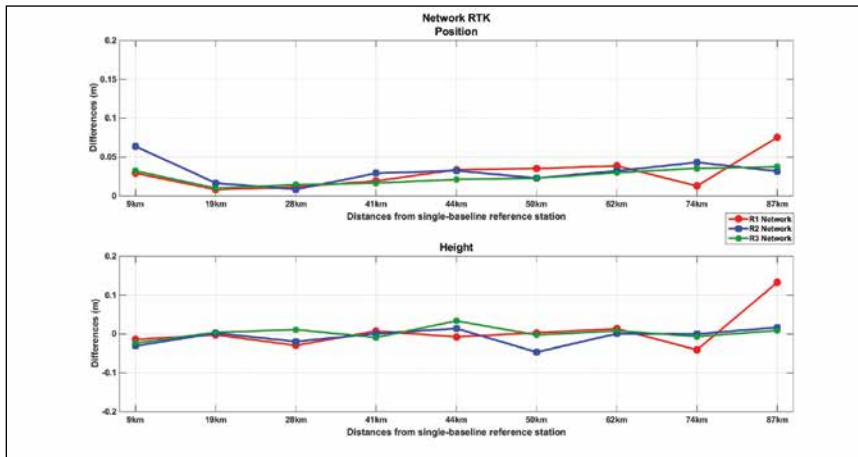

Figure 3. Differences between known and network RTK–derived coordinates

Turkish RTK Continuously Operating Reference Station (TUSAGA-Aktif) Network points, i.e. CORU (40^0.57041 N; 34^0.98220 E), SUNL (40^0.15398 N; 34^0.36891 E), YOZ1 (39^0.83144 N; 34^0.84473 E), AKDG (39^0.66016 N; 35^0.87164 E), AMAS (40^0.66569 N; 35^0.84929 E) were chosen as reference stations and the coordinates of the established 27 points were calculated with carrier-phase-based relative method by using Leica Geosystems commercial GNSS post-processing software. The necessary data for those reference stations were downloaded from the TUSAGA-Aktif's data archives (http://rinex.tusaga-aktif.gov.tr).

The test measurements were carried out with multi-frequency and multi-constellation Trimble R10 GNSS receivers. Some prominent technical features of the receivers are given in Table 2.

The RTK-derived coordinates were compared with those of the differential technique results (known coordinates) and differences in <*2D position*> and <*height*> components are given in Figure 2 for Single Baseline RTK positioning and in Figure 3 for Network RTK positioning. All differences with statistical results are tabulated and given in Table 3.

When the obtained results given in Figure 2 and 3 and Table 3 are examined, it can be seen that, both methods provide real-time positioning with cm to dm level of accuracy. However, maximum differences were obtained for both approaches in the group of measurements which were held at 87 km from the base station of the Single Baseline RTK (8 cm in position for Network RTK and 20 cm in position for Single Baseline RTK). This has been observed in only one of the 3 points surveyed. Thus, it can be stated that these big differences are obtained occasionally.

In general, the study shows that with the Network RTK approach, more homogeneous accuracy can be achieved (few cm level of accuracy in 2D position and height components with a few exceptions,). By using Single Baseline approach, the 2D position and height can be determined with less than dm level of accuracy in the measurements of all groups except the point group at 87 km distance away Single Baseline reference station.

Conclusion

In this study the performance of Single Baseline and Network RTK systems were evaluated and the attainable static accuracies were compared to each other. The results show that, although Network RTK performs more homogenous and more accurate results when compared to Single Baseline RTK, both approaches provide positioning with a few cm-level of accuracy when the fix solution is obtained.

In general, the results indicate that both Single Baseline and Network RTK-derived coordinates agree with the relative positioning solution at a few cm level of accuracy in both 2D position and height components. The RTK users make their continuous real-time positioning very reliable, fast (typically in few minutes), cost-effective within cm- to dm level of accuracy. Based on this study it can be concluded that, the Single Baseline or Network RTK approaches are an attractive alternative to conventional relative positioning method that require expensive and time-consuming field and office processes.

On the other hand, although RTK systems, especially Network RTK, are being used more widely in different projects each day due to their several advantages, need for base stations with enough density, need for a communication link (GSM, Wi-Fi, Internet, etc.) more complicated and more expensive equipment and infrastructure requirements, difficulties in continuous operation and labor, operating costs, etc., are the restricting factors in such systems.

References

Alkan, R.M., *Ozulu, I.M.,* Ilci, V., *Tombus*, F.E. and *Şahin, M. (2017). Usability of GNSS Technique for Cadastral Surveying. In: T.* Yomralioglu *and J.* McLaughlin*, eds., Cadastre: Geo-Information Innovations in Land Administration, 1st ed., New Delhi: Springer International Publishing, pp. 77-91.*

Aponte, J., Meng, X. and Burbidge, M. (2008). Performance Assessment of a GPS Network RTK Service. In: *FIG Working Week 2008*, Stockholm, Sweden.

Bakıcı, S. and Mekik, C. (2014). TUSAGA-Aktif: Delivering Benefits to Turkey. *Coordinates*, X(2), pp. 19-26.

Bakıcı, S. (2015), Geoinformatik Teknolojilerinin Tapu ve Kadastro Genel Müdürlüğünde Kullanımı. *1. Konum Belirleme ve Uydu Navigasyonu Zirvesi-2015*, Istanbul, Turkey (In Turkish).

Cina, A., Dabove, P., Manzino, A.M. and Piras, M. (2015). Network Real Time Kinematic (NRTK) Positioning-Description, Architectures and Performances. In: J. Shuanggen, ed., Satellite Positioning-Methods, Models and Applications, InTech Publishing, pp. 23-45.

Denys, P. and Pearson, C. (2016). Positioning in Active Deformation Zones-Implications for NetworkRTK and GNSS Processing Engines. FIG Article of the Month-March 2016. http://www.fig.net/resources/monthly_articles/2016/denys_pearson_march_2016.asp [Accessed 15 Nov. 2017].

El-Mowafy, A. (2012). Precise Real-Time Positioning Using Network RTK. In: J. Shuanggen, ed., *Global Navigation Satellite Systems: Signal, Theory and Applications*. InTech Publishing, pp. 161-188.

Eren, K., Uzel, T., Gulal, E., Yildirim, O. and Cingoz, A. (2009). Results from a Comprehensive Global Navigation Satellite System Test in the CORS-TR Network: Case Study. *Journal of Surveying Engineering*, 135(1), pp. 10-18.

Fotopoulos, G. and Cannon, M.E. (2001). An Overview of Multi-Reference Station Methods for cm-Level Positioning. *GPS Solutions*, 4(3), pp. 1-10.

Kahveci, M. (2009). Real Time Continuously Operating Reference Stations (RTK CORS) Networks and Considerations About Them. *HKM Jeodezi, Jeoinformasyon ve Arazi Yönetimi Dergisi*, 1(100), 13-20 (in Turkish).

Kim, H.H., Sung, Y.M. and Lee, J.H. (2017). GNSS CORS and Network-RTK Service in Korea. In: *2017 IGS Workshop*, University of Paris-diderot in Paris, Paris, France.

Lachapelle, G. and Alves, P. (2002). Multiple Reference Station Approach: Overview and Current Research. *Journal of Global Positioning Systems*, 1(2), pp. 133-136.

Mekik, C., Yıldırım O. and Bakıcı, S. (2011). The Turkish Real Time Kinematic GPS Network (TUSAGA-Aktif) Infrastructure. *Scientific Research and Essays*, 6(19), pp. 3986-3999.

Ogutcu, S. and Kalaycı, I. (2016). Investigation of Network-based RTK Techniques: A Case Study in Urban Area. *Arabian Journal of Geosciences*, 9(3), pp. 1-12.

Prochniewicz, D., Szpunar, R. and Walo, J. (2017). A New Study of Describing the Reliability of GNSS Network RTK Positioning with the Use of Quality Indicators. *Measurement Science and Technology*, 28(1).

Rizos, C. (2002). Network RTK Research and Implementation-A Geodetic Perspective. *Journal of Global Positioning Systems*, 1(2), pp. 144-150.

Rizos, C. (2007). Alternatives to Current GPS-RTK Services and Some Implications for CORS Infrastructure and Operations. *GPS Solutions*, 11(3), pp. 151-158.

Wanninger, L. (2006). *Introduction to Network RTK*. IAG Working Group 4.5.1: Network RTK (2003-2007).

URL 1. *Trimble R10 GNSS System*, Available at: https://geospatial.trimble.com/products-and-solutions/r10 [Accessed 15 Nov. 2017].

In this study the performance of Single Baseline and Network RTK systems were evaluated and the attainable static accuracies were compared to each other. The results show that, although Network RTK performs more homogenous and more accurate results when compared to Single Baseline RTK, both approaches provide positioning with a few cm-level of accuracy when the fix solution is obtained

Crowd monitoring through WiFi data

A methodology has been developed and tested using real data. The data were collected during the JRC Open Day 2016 by 20 WiFi access points deployed on the Ispra site

Ciro Gioia
Scientific/Technical Project Officer, European Commission, Joint Research Centre (JRC), Directorate for Space, Security and Migration, Demography, Migration & Governance Unit, Ispra (VA), Italy

Francesco Sermi
European Commission, Joint Research Centre (JRC), Directorate for Space, Security and Migration, Demography, Migration & Governance Unit, Ispra (VA), Italy

Dario Tarchi
Senior Expert, European Commission, Joint Research Centre (JRC), Directorate for Space, Security and Migration, Demography, Migration & Governance Unit, Ispra (VA), Italy

Michele Vespe
Scientific Officer, European Commission, Joint Research Centre (JRC), Directorate for Space, Security and Migration, Demography, Migration & Governance Unit, Ispra (VA), Italy

The capability to monitor the gathering of crowds in restricted geographic areas is a key enabler for the development of safety and security measures. The knowledge of the people flows within streets, squares, neighbourhoods and buildings could help preventing critical concentrations in bottlenecks, supporting the deployment of emergency services staff and developing services for smart cities [1]. Besides, for common places of gathering such as parks or stadiums, this information would improve the positioning of commercial and customer targeted services.

There are various methods to estimate the number of presences in a given area:

1. physical counting in strategic points;
2. Jacob's method based on the size of the area where the event is organized (2-4 peoples for squared meter) [2];
3. employment of automated systems.

To date, most of the crowd monitoring techniques rely on camera networks, satellite images, or mobile phones data [3]. The first two approaches are relatively expensive, require complex image processing [4] and are limited to daylight and visibility operations; while, the third method requires data from telecom providers and faces strong privacy constraints which limit its application [5].

In this paper, an approach based on WiFi data is proposed: stations belonging to a network collect WiFi-related data of mobile devices. A pilot has been recently developed by Transportation for London (TfL), which is currently limited on the collection of WiFi data [6], exploring main privacy issues.

Whenever the WiFi connectivity of a mobile device is active, the device periodically broadcasts probe requests to associate to a network. The probe request is a frame used to request information to the Access Point (AP); the request includes, among other information, the Media Access Control (MAC) address, which is a unique identifier of the device. All these records can be seen as a footprint: despite the owner of the footprint is unknown, by counting the different footprints one can estimate how many people passed by. In this way, mobile devices can be counted without encroaching on the privacy of their owners. A more detailed discussion about the privacy can be found in [7]. In those terms, the crowd monitoring seems quite simple. Yet a positioning algorithm, preceded by an *ad hoc* data cleaning, is required.

The approach introduced [7] was tested in occasion of the Open Day 2016 at the Joint Research Centre (JRC) Ispra site, in Italy [8]. During the event, 20 WiFi APs, spread within the perimeter of the site, recorded the presence of mobile devices; the collected data allowed the estimate of the number of visitors and their flow. The unique data set allows the validation of the results, which usually is a weak point of the big-data analysis. Specifically, the estimated number of visitors is compared to the data provided by the security service; whereas, the flow monitoring is validated through the schedule of the event.

The JRC open day experiment

The JRC Open Day 2016 in Ispra took place on Saturday the 28th of May. The

event attracted about 8000 visitors. Thanks to its large area (167 hectares) and its restricted-access nature (only one controlled access for visitors), the event represented a unique test bench for the validation of the proposed crowd monitoring method.

Figure 1 shows the positions of the 20 devices within the site. Three main areas are identified with a different colour of the APs: the entrance (blue), the central part (yellow) and the exit (red). Among the blue stations, numbers 10 and 11 were positioned at the visitors' entrance, whereas station 12 was placed in the proximity of the access reserved to volunteers. Device 16, in the upper-right part of the map, was positioned at the secondary entrance, which was active only for few hours and reserved to volunteers entrance. All the APs where activated before the opening of the event; some of them were previously activated and then positioned, as it can be seen from the results presented in section 4. The APs continuously recorded data during the entire event. Only few of them failed working during the day, without affecting the final result of the experiment.

Algorithm description

In this section, the algorithm developed to monitor people flow is described. The algorithm is divided in

Figure 1: Displacement of the 20 APs on the JRC Ispra site. The devices continuously logged data during the 2016 JRC open day
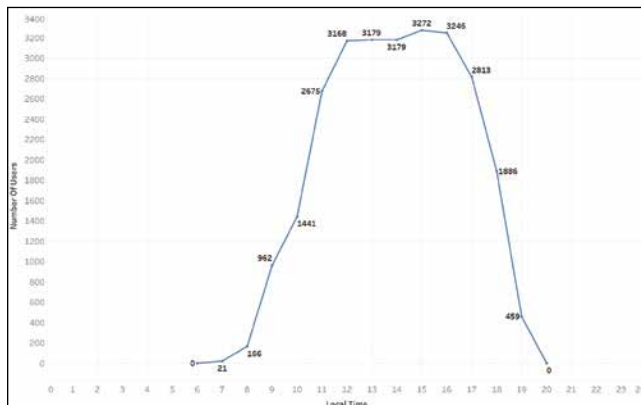

Figure 2: Number of unique users as a function of the local time

two phases namely Cleaning and Localization. The two phases are described in the following sections.

Cleaning procedure

If a WiFi network is deployed over a specific area, as in the 2016 JRC open day, the number of user in the area can be estimated as the number of unique MAC address connected to the network. However, such estimate can be a challenge because it is affected by three main problems: the presence of random generated MAC address [9], the inclusion of people that are not attending the event but are in the proximity of the APs and the inclusion of static devices (printers, PCs etc.). In order to mitigate such effects, two criteria to identify a "*real user*" are applied (see eq. 1). The first criterion is based on the minimum number of records (in our case 3) associated to a specific MAC address; this criterion allows the exclusion of random generated MAC address which are used by some manufacturers to verify the availability of WiFi networks; After this check such devices connect to the network using the real MAC. The second criterion considers the minimum number of stations where a specific user is recorded (the threshold used was 3, according to the topology of the deployed network); this criterion allows the exclusion of people seen only by a limited number of stations and also excludes static devices which are connected to a limited number of APs.

$$real\ user = \begin{cases} Criterion\ 1\ (user\ recorded\ at\ least\ 3\ times) \\ \& \\ Criterion\ 2\ (user\ recoded\ at\ least\ by\ 4\ stations) \end{cases} \quad (1)$$

Localization

In order to estimate the distribution of the people on the site, the location of the real users is required; the localization is attempted using an algorithm based on the *centroid principle*. The classical centroid algorithm computes the position of the user as the mean of the station coordinates at which the user is simultaneously connected. In our case, there was a limited overlapping of the station coverage, hence the classical centroid converges to the proximity solution. To overcome this limitation a modified Weighted Centroid (WeC) approach has been implemented. The position of the user is computed as the mean of the station coordinates at which the user is connected in a specified time interval (eq. 2) weighted by the Receiver Signal

Strength (RSS) (eq. 3): $P_u(x_u,\ y_u, \Delta t\ ) = \frac{\sum_{i=0}^{N-1} w_i P_i}{\sum_{i=0}^{N-1} w_i}$ (2)

P_i is the position of the ith station, Δt is the considered time interval (3 minutes in our case) and w_i is the weight of the the position of the ith station which is defined as: $w_i = \dfrac{1}{2 \cdot 10^{-RSSI_i/_{10}}}$ (3)

Results

In this section, the main results are summarized: at first, the estimated number of presence is provided, then the distribution of presence during the event is computed. Moreover,

statistics on the number of users recorded are provided; the concentration of people is disaggregated by stations and time.

The estimated number of users without applying any cleaning was some 50000, which is reduced to 7143 after the application of the criteria described in section 3.1. This number underestimates by some 6% the presences on the site, since the security office reported 7623 accesses during the entire event. Such a reasonable discrepancy can be attributed to the presence of children without any device and of users with WiFi connection turned off.

The number of real users disaggregated by hours is shown in Figure 2; from the figure it can be noted that the number of users slowly raised between 6:00 and 8:00, when only volunteers were allowed to enter. Then, between 9:00 and 12:00, there is a fast growth of the number of visitors which is compatible with the actual event schedule. In fact, in spite the opening was scheduled for 10:00, the security office decided for an early opening of the site at 9:00, facilitating the inflow of the people. Between 12:00 and 16:00, the number of people on site remained almost constant, registering only a small increase between 14:00 and 15:00, which is also confirmed by the security report. Finally, after 16:00, the total number of visitors started rapidly to decrease, confirming the fact that people were leaving when the closure of the event (scheduled at 17:30) was approaching.

In Figure 3, the estimated number of people entering the site using the proposed approach is compared with respect the number of people registered by the security service at the main gate. From the figure it appears that the number of people registered by the security (blue area) is similar to the estimate obtained using the proposed methodology (red area). Only in the first hour a significant difference can be appreciated, this phenomenon is probably due to the fact that between 8:00 and 9:00 only volunteers were allowed to enter the site and they were not registered by the security service. The maximum number of people entering the site was 57 form the official statistics of the security office ant it occurs at 10:00 approximately; whereas the proposed methodology estimated that the maximum number of people entering the site was 59 a bit before 11:00.

In order to analyze the distribution of the people on the site during the event, the total number of users recorded by each station is shown in Figure 4. From the figure, it can be noted how the minimum value (47 users) was registered by the AP located in the proximity of the secondary gate reserved to volunteers' entrance, which remained open only for few hours. On the contrary, the highest number of users (i.e. 3949) was recorded by the station in the center of the site, which was located in the proximity of a bus stop. Moreover, the number of users recorded by close stations is very similar; for example, the difference between the number of users registered by two APs located on two side of the same block (stations 15 and 24) was only four.

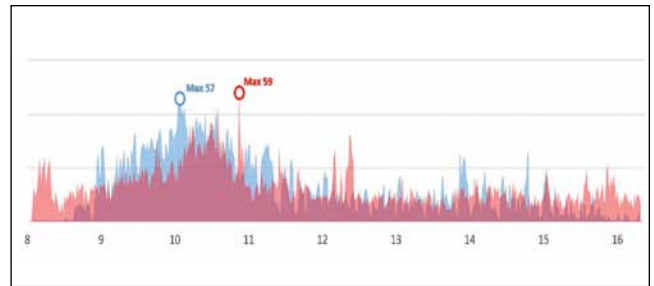The median time spent by the users in each station is shown

Figure 3: Number of unique users as a function of the local time
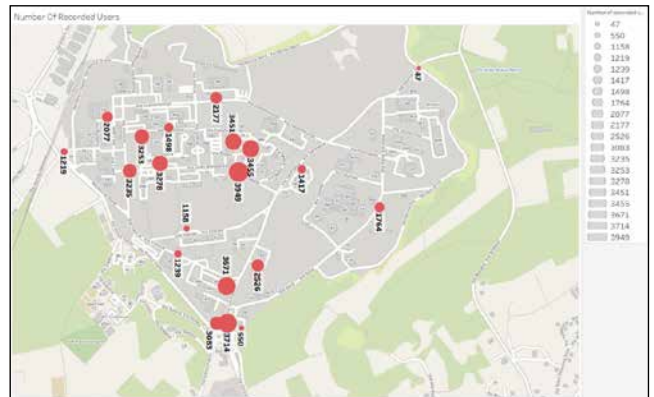
Figure 4: Number of real users recorded by each station
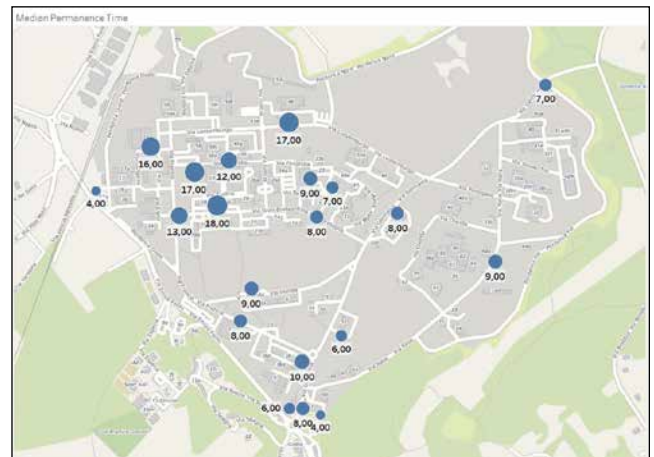
Figure 5: Median permanence time in the different stations
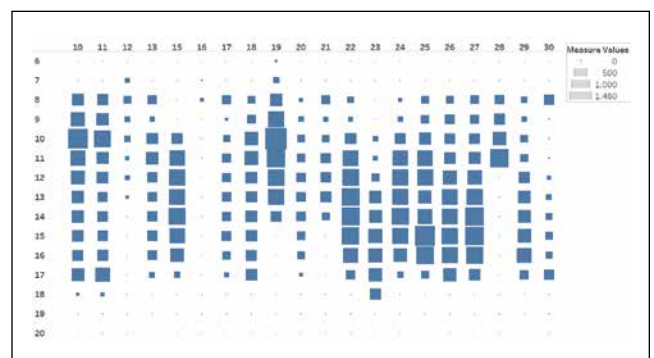
Figure 6: Number of users in the different stations during the event

in Figure 5. The permanence time in the proximity of the entrance can be considered the time waiting to enter the site; it can be noted that volunteers (4 minutes) were faster in accessing the site than the general public (8 minutes). The time spent by the visitors in the proximity of the main exhibitions (stations 23, 25, 26, 27 and 29) ranges between 13 and 18 minutes.

The number of real users, breakdown by hours and stations, is represented by the size of the squares in Figure 6. APs number 12, 16 and 19 were the only recording users before the opening of the site. Station 12 and 16 were in the proximity of the two gates reserved for the access of the volunteers, whereas AP 19 was located in the proximity of an exhibition which was installed very early in the morning. Station 10 and 11, located in the proximity of the visitor entrance, have a very similar behavior: the number of users increase in the first hours, then it decreases in the afternoon, to increase again around 17:00, when the event was officially closed and the gate was opened to allow the exits of volunteers. Finally, it can be noted that station 28 stopped working after 11:00.

In order to further demonstrate the effectiveness of the proposed approach, the flow of people in stands opened to a closed-number of participants (only 40 at time) is

The estimated number of attending people were compared with the statistics of the security service showing evident consistency; the possibility to validate the results with independent information represents a significant added value to this research.

considered. Different groups of people entered he Visitors' Centre (station 17) every 30-minutes, from 11:00 to 17:00. The time trend of the estimated number of users recorded by the AP in the proximity of the Visitors' Centre is shown in Figure 7. The high consistency between the estimated number of real users and the schedule of the event clearly emerges. The peak at 8:30 correspond to the installation phase, when the staff was setting up the exhibition.

Finally, the distribution of the people on the site between 10:00 and 11:00 (after the official opening of the event) is shown in Figure 8. From the figure, the following

conclusions can be deduced: the maximum concentration of people is recorded in the proximity of the main gate (stations 10, 11 and 12); a considerable number of users were already in the central part of the site, probably because of the early opening at 9:00; only few users were in the proximity of the exit area (between stations 26, 29 and 30); no presences were detected in proximity of station 16.

Conclusions

The research pointed out the feasibility of crowd monitoring through WiFi positioning. The huge amount of data gathered during the JRC Open Day 2016 by 20 WiFi access points deployed within the Ispra site were cleaned and processed to analyse people flow and estimate the number of participants to the event. The cleaning procedure allowed the identification of actual users among all the registered MAC addresses. Such cleaning was divided into two steps: exclusion of random generated MAC addresses (iOS based systems, etc.); exclusion

of MAC addresses recorded only by a limited number of stations (people detected by the perimeter stations that did not entered the site and static devices). The data processing is basically a positioning procedure carried out through a modified WeC approach that exploits the RSS as waiting factor.

The results of the experiment were compared with the report from the security service and with the actual schedule of the event, showing evident consistency. Although the data analysis was carried out off-line, the proposed method clearly adapts to a quasi-real time application, since only a small time interval is required for data cleaning and processing. Hence it fully fits needs of the deployment of emergency services staff and of the developing services for smart cities.

References

[1] P. Bellini, D. Cenni, P. Nesi, I. Paoli "Wi-Fi based city users' behaviour analysis for smart city", Journal of Visual Languages & Computing, Volume 42, 2017, pp 31-45.

[2] H. Jacobs "To count a crowd" 1967, Columbia Journalism Review, Volume 6, pp 36-40.

[3] Y. Yuan, "Crowd Monitoring Using Mobile Phones," 2014 Sixth International Conference on Intelligent Human-Machine Systems and Cybernetics, Hangzhou, 2014, pp. 261-264.

[4] A.N. Marana, S.A. Velastin, L.F. Costa and R.A. Lotufo, "Estimation of crowd density using image processing", IET Conference Proceedings, 1997, p. 11.

[5] European Commission, "EU Directive 95/46/ec - The Data Protection Directive," tech. rep., European Commission, 2016.

[6] Transport for London (TfL) "WiFi data collection pilot" https://tfl.gov.uk/corporate/privacy-and-cookies/wifi-data-collection-pilot

[7] A. Alessandrini, C. Gioia, F. Sermi, I. Sofos, D. Tarchi and M. Vespe, "WiFi positioning and Big Data to monitor flows of people on a wide scale," 2017 European Navigation Conference (ENC), Lausanne, 2017, pp. 322-328.

[8] https://ec.europa.eu/jrc/sites/jrcsh/files/jrc-ispra-openday-2016-map-programme_en.pdf

[9] M. Vanhoef, C. Matte, M Cunche, L.S. Cardoso and F. Piessens "Why MAC Address Randomization is not Enough: An Analysis of Wi-Fi Network Discovery Mechanisms" ACM Asia Conference on Computer and Communications Security, (ASIACCS 2016), 2016 China.
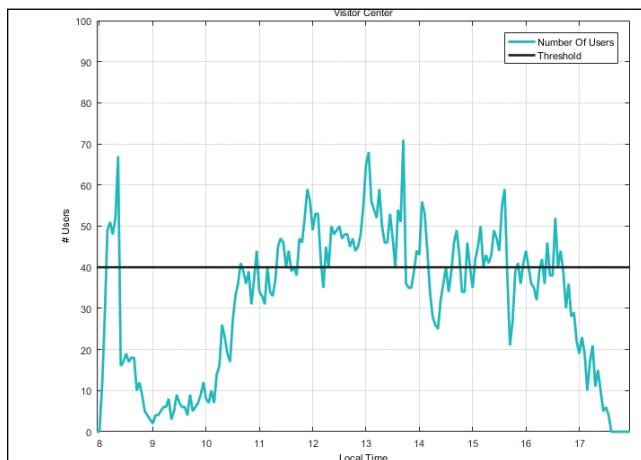
Figure 7: Number of users recorded by the AP number 17 in the proximity of the Visitors' Centre

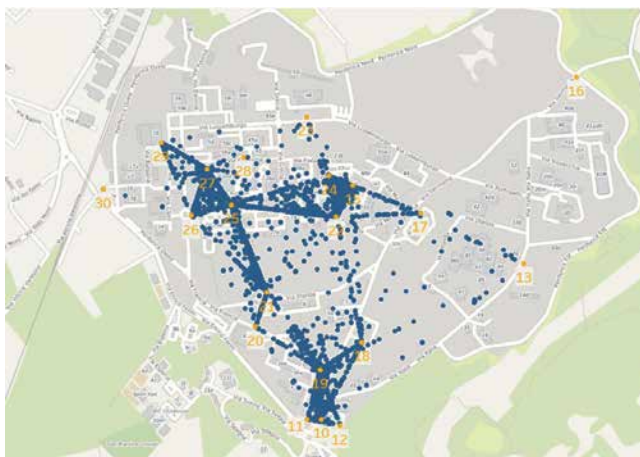**Figure 8: Distribution of the users on the JRC Ispra site during the 2016 JRC open day. Considered time interval 10:00–11:00**

Are administrative boundaries in Google maps correct?

Google maps are extensively used now-a-days in various scientific applications. However the question of accuracy of the maps needs to be explored especially when dealing with the political boundaries or borders between states or nations.

S. Vasantha Kumar
Associate Professor,
School of Civil and
Chemical Engineering,
VIT University, Vellore,
Tamil Nadu, India

In recent years, 'Google Maps' become the most widely used open source web based mapping application as it provides high resolution satellite imagery, street level cartographic maps, panoramic views of streets, real time traffic information and shortest travel route by private or public transportation in any part of the world. The high resolution maps and satellite imagery from Google maps are extensively used by the scientific community to study urban landuse changes[1, 2], detect oil palm plantations[3], delineate cropland[4] and agriculture areas[5], measure landscape attractiveness[6], locate crime hotspots[7], evaluate walking distances for vascular claudication patients[8], dengue surveillance system[9], etc. Though Google maps are used in various scientific applications, however the question of accuracy of the maps needs to be explored especially when dealing with the political boundaries

or borders between states or nations. As a pilot study, the state boundary from Google maps are compared with that of Survey of India (SOI) toposheets for a sample area to check whether the boundaries shown in Google maps are matching with that of toposheets or not. Six toposheets numbered 57O/4, O/8, K/16, L/13, P/1, P/5 covering Vellore district in Tamil Nadu and Chitoor district in Andhra Pradesh was obtained from Survey of India Nakshe portal[10].

The toposheets were georeferenced using the known latitude and longitude values and were mosaicked to form one single image. It was then converted from geographic coordinate system (latitude/longitude) to projected coordinate system (northing/easting) using Universal Transverse Mercator (UTM) projection in Arc GIS 10 software. Onscreen digitizing of the boundary between the
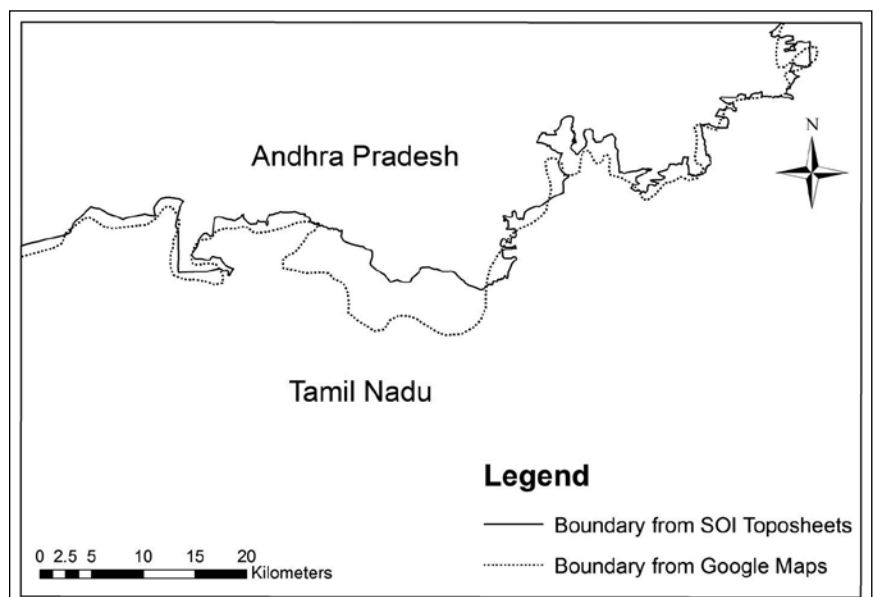
Figur.1 Map showing the state boundary from SOI toposheets and Google maps

Present study compared the Political Boundaries in Google maps with that of Survey of India toposheets. Results indicates that Google maps fail to depict the political boundaries correctly and thus suggests that the scientific community need to be careful while using Google maps especially when dealing with borders or political boundaries between states.

two states was manually done. Google map covering within the toposheets was imported as image file and georeferenced using the SOI toposheet through image to image registration. Locations which can be identified in both toposheet and google map such as road intersections, railway crossings were considered during image to image registration.

After georeferencing, Google maps were projected to the UTM coordinate system and the state boundary was manually digitized. From the results shown in Fig.1, it can be seen that there is a mismatch between the boundaries and the Google map boundary does not follow the true boundary shown in SOI toposheets.

The actual boundary from SOI toposheets measures a length of 199.647 km whereas the Google map boundary measures only 150.500 km. Almost 50 km length has been missing in Google maps for this sample area itself. Because of the discrepancy in lengths between the toposheet and Google map, the area covering within the states also differs dramatically. For example, the true area of Tamil Nadu covering within these toposheets is 3168.8 sq.km, whereas the area from Google

maps is only 3034.54 sq.km. Similarly in Andhra Pradesh, the area measured from toposheets is 1329.743 sq.km whereas in Google maps it is 1464.003 sq.km.

The results indicates that Google maps fail to depict the political boundaries correctly and thus suggests that the scientific community need to be careful while using Google maps especially when dealing with borders or political boundaries between states.

References

[1] Malarvizhi, K., Vasantha Kumar, S. and Porchelvan, P., Use of high resolution google earth satellite imagery in landuse map preparation for urban related applications. Procedia Technology, 2016, 24, 1835 – 1842.

[2] Jacobson, A., Dhanota, J., Godfrey, J., Jacobson, H., Rossman, Z., Stanish, A., Walker, H. and Riggio, J., A novel approach to mapping land conversion using Google Earth with an application to East Africa. Environmental Modelling & Software, 2015, 72, 1 -9.

[3] Lee, J., Wich, S., Widayati, A. and Koh, L., Detecting industrial oil palm plantations on Landsat images with Google Earth Engine. Remote Sensing Applications: Society and Environment, 2016, 4, 219–224.

[4] Xiong, J., Thenkabail, P., Gumma, M., Teluguntla, P., Poehnelt, J., Congalton, R., Yadav, K. and Thau, D., Automated cropland mapping of continental Africa using Google Earth Engine cloud computing. ISPRS Journal of Photogrammetry and Remote Sensing, 2017, 126, 225-244.

[5] Pulighe, G. and Lupia, F., Mapping spatial patterns of urban agriculture in Rome (Italy) using Google Earth and web-mapping services. Land Use Policy, 2016, 59, 49-58.

[6] Vries, S., Buijs, A, Langers, F., Farjon, H., Hinsberg, A. and Sijtsma, F., Measuring the attractiveness of Dutch landscapes: Identifying national hotspots of highly valued places using Google Maps. Applied Geography, 2013, 45, 220-229.

[7] Vandeviver, C., Applying Google Maps and Google Street View in criminological research. Crime Science, 2014, 3(13), 1-16.

[8] Khambati, H., Boles, K. and Jetty, P., Google Maps offers a new way to evaluate claudication. Journal of Vascular Surgery, 2017, 65(5), 1467-1472.

[9] Chang, A., Parrales, M., Jimenez, J., Sobieszczyk, M., Hammer, S., Copenhaver, D. and Kulkarni, R., Combining Google Earth and GIS mapping technologies in a dengue surveillance system for developing countries. International Journal of Health Geographics, 2009, 8, 1-11.

[10] http://www.soinakshe.uk.gov.in

MULTIPATH BUSTERS
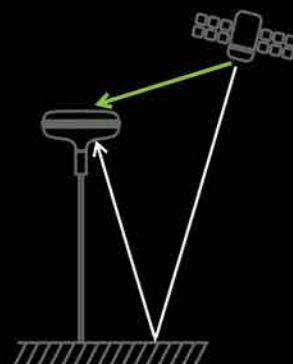
Multipath appears like a **ghost signal** that degrades the accuracy of your shots. We **detect and bust** these ghosts by sophisticated signal processing techniques in our **TRIUMPH** chip. We also show the **signature** of these ghosts that we bust. Below are two screenshots from the TRIUMPH-LS.

SAT	EL	AZ	L1	P1	P2	L2C	L5
GPS2	29↑	154	7	7	2	--	--
GPS6	44↑	98	11	9	2	2	-13
GPS12	70↑	282	7	8	-2	-2	--
GPS14	25˙	302	5	8	-4	--	--
GPS17	23↓	58	6	9	-6	-2	--
GPS24	53↓	196	1	4	13	1	-12
GPS25	30↑	282	4	8	7	1	-32
GLN1	10↑	34	1	4	-15	-23	--
GLN8	16↓	344	12	15	17	25	--
GLN9	32↑	316	0	2	-3	-6	--
GLN15	31↓	142	5	5	0	1	--
GLN16	84↑	266	2	2	-11	-18	--
GLN17	39↓	44	-1	-4	-12	-10	--
GLN18	69↑	188	-1	3	-1	-6	--
GAL12	68˙	108	0	-26	0	--	-14
SB127	25˙	160	7	--	--	--	-4
SB128	15˙	130	9	--	--	--	-11
QZ193	13↑	68	-3	-1	--	1	-19
BDU2	16˙	132	-7	--	--	--	-17
BDU5	25˙	154	-4	--	--	--	-7
BDU8	25↓	54	-10	--	--	--	-20

SAT	EL	AZ	L1	P1	P2	L2C	L5
BDU11	75↑	158	-6	--	--	--	-5
BDU12	36↓	60	-6	--	--	--	-14
GPS3	10	26	--	--	--	--	--
GPS29	3	229	--	--	--	--	--
GPS32	3	346	--	--	--	--	--
GLN7	3	297	--	--	--	--	--
GLN19	12	210	--	--	--	--	--

SAT	EL	L1	P1	P2	L2C	L5
GPS2	29↑	273	281	-76	--	--
GPS6	44↑	55	201	-60	-5	189
GPS12	70↑	183	190	-90	-94	--
GPS14	25˙	281	317	-97	--	--
GPS17	23↓	332	364	-74	6	--
GPS24	53↓	117	566	67	-64	124
GPS25	30↑	243	218	-42	-50	-34
GLN1	10↑	305	229	-126	-404	--
GLN8	16↓	26	87	-484	-617	--
GLN9	32↑	359	301	-246	55	--
GLN15	31↓	276	203	-93	-2	--
GLN16	84↑	235	309	-133	-109	--
GLN17	39↓	52	-84	-156	-52	--
GLN18	69↑	190	168	-177	-184	--
GAL12	68˙	680	-121	246	--	32
SB127	25˙	469	--	--	--	319
SB128	15˙	206	--	--	--	322
QZ193	13↑	550	513	--	56	55
BDU2	16˙	299	--	--	--	275
BDU5	25˙	269	--	--	--	230
BDU8	25↓	145	--	--	--	143

SAT	EL	L1	P1	P2	L2C	L5
BDU11	75↑	362	--	--	--	305
BDU12	36↓	288	--	--	--	200
GPS3	10	--	--	--	--	--
GPS29	3	--	--	--	--	--
GPS32	3	--	--	--	--	--
GLN7	3	--	--	--	--	--
GLN19	12	--	--	--	--	--

In each column the relative amount of multipath ghosts that has been detected and busted from each signal **carrier phase** is shown (in millimeters). In the carrier phase it is up to a **quarter of a cycle** (wavelength).

In each column the relative amount of multipath ghost that has been detected and busted from each signal **Code phase** (range) is shown (in centimeters). In the code phase it is approximately **several meters**.

Verify, Monitor, Record, Present and Defend

RTK is a statistical process by nature and needs **verification**. TRIUMPH-LS has **six different RTK engines** and extensive automatic verification to ensure your shots are 100% reliable (see www.javad.com).

It also has many tools to **document** the process of your shots for **presentation** when you need to **prove** and **defend**. The screenshots can automatically be recorded and attached to each point and easily **exported to HTML format**.

Single Point Localization

Surveyors often find it more convenient to work with a custom coordinates system than a predefined projection, such as SPCS or UTM. The reasons may be many, but often it is desirable to utilize a coordinate system with a low scalar difference from ground based measurements or to have the bearing relation closer to geodetic North.

The Localization application in J-Field on the TRIUMPH-LS is capable of producing useful Low Distortion Projections in seconds. The application is producing a new Oblique Stereographic or Transverse Mercator projection.

J-Tip
Integrated Magnetic Locator

$850

No need to carry heavy magnetic locators any more. The J-Tip magnetic sensor replaces the tip on the bottom of your rover rod/monopod. Its advanced magnetic sensor send 100 Hz magnetic values to the TRIUMPH-LS via Bluetooth. TRIUMPH-LS scans the field and plots the 2D, 3D and time view of magnetic characteristics. It also shows the shapes and the centres of the objects under the ground and guides you to it.

PATENTS PENDING

J-Tip advantages:

• J-Tip does not have "null" points around the peak and will not produce false alarms.

• J-Tip is fully automatic for all levels of magnets. There is even no "Gain" button to adjust.

• J-Tip senses the mag values in all directions. You don't need to orient it differently in different searches.

• J-Tip gives a 2D and 3D view of the field condition when you have RTK and will guide you to the object. You can actually see the shape of buried object.

• J-Tip, In Time View, shows positive and negative mag values of the last 100 seconds and the Min and the Max since Start.

• J-Tip shows the instantaneous magnetic vector in horizontal and vertical directions.

• J-Tip works as a remote control for the TRIUMPH-LS

• J-Tip weighs 120 grams and replaces the standard pole tip. In balance, it weighs almost nothing.

• The built in camera of the TRIUMPH-LS documents the evidence after digging.

• And... you don't need to carry another bulky device.

J-Pod $850
A rugged Transformer-Pod

J-Pack $290
Convenient survey bag

Javad......Bravo!!!!

The J-Pack is nicest bag I have ever seen for surveying. I especially like the pocket in the back and all of the places to tie down equipment and stuff.

Adam Plumley, PLS

J-Pod Inside bag.

Monopod >>> to + Bipod >>> to + Tripod…
# On demand.

Who moved my ⚐ base?

It is well known that having your own base station near your job site provides you with faster, more accurate, more reliable and less expensive solutions. If you don't know the accurate position of your base, our DPOS service will find it. Read details in the following pages.

After you start your base, If during your survey somehow your base is moved, all your rover points will be inaccurate to the amount of the base movement. But...

...But! Don't Worry, Be Happy:

We will let you know instantly during your survey if your base has moved. We use:

1. Inclinometer which shows the tilt value.

2. Accelerometer which shows motion and shocks.

3. We calculate displacement. This value is accurate to 2 cm.
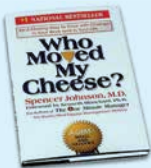
By the way, a must read book for adult professionals

1) Set the displacement threshold here. "Off" means ignore displacement. Our default is 5 cm.

2) Click the "Start Base". it will change to "Stop base."
RTK corrections as well as motion values will be transmitted to the rover. Maximum values of the motion parameters will be kept at all time.

3) Maximum values of the three sensors can be shown in a white box in the action screen. Top left is the acceleration in milliG, bottom left is tilt and bottom right is displacement in centimeter.

4) If any of the threshold values exceeds, a pop up will alert you and shows the maximum value of the sensors since you started the base. The bottom number is time since the threshold(s) exceeded.

5) To setup for base movement alert, go to base rover setup screen and click on the left side of the screen.

6) You can set up threshold limits for accelerometer, inclinometer (tilt) and displacement values to create alert when these thresholds are exceeded.

7) Set Acceleration limit here. The units are in milliG (mG). G is acceleration in free fall. "Off" means ignore this sensor. Our default is 5 mG

8) Set the tilt threshold here. Units are in degree. "Off" means ignore tilt. Our default is 5 degrees.
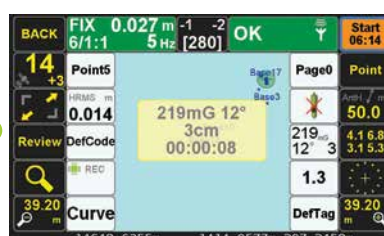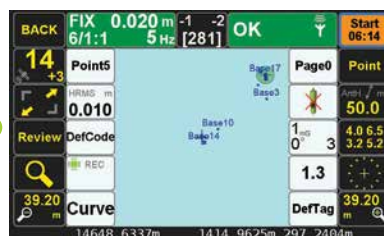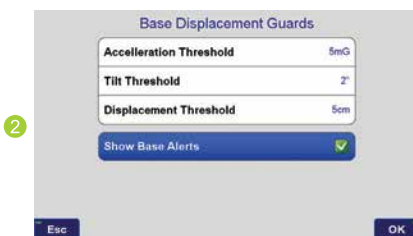
Receivers

TRIUMPH-1M

$8,990

864 channel chip, equipped with the internal 4G/LTE/3G card, easy accessible microSD and microSIM cards, includes "Lift & Tilt" technology.

TRIUMPH-2

L1 $1,990

L1/L2 $3,490

with RTK $4,990

Total 216 channels: all-in-view (GPS L1/L2, GLONASS L1/L2, SBAS L1) integrated receiver.

The one and the only Digital Radio Transceiver in the world!

Unique adaptive digital signal processing, which has benefits: the full UHF frequency range and all channel bandwidths worldwide • the best sensitivity, dynamic range, and the highest radio link data throughput • embedded interference scanner and analyzer • compatibility with another protocols. Cable free Bluetooth connectivity with GNSS receivers and Internet RTN/VRS access via embedded LAN, Wi-Fi, and 3.5G
*Power, data cables and antenna are included.

And all this with competitive prices!

Cellular antenna

GNSS antenna

RGB LED indication

BT/WiFi antenna

SIM card and microSD card slots

DB26 connector

Power connector

JLINK LTE*

$1,499
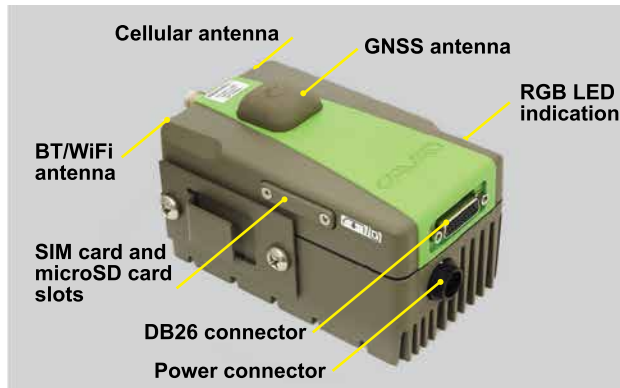
Connects all types of devices via UHF, WiFi, Bluetooth, and 4G/LTE for reliable IP communication in the field.

HPT401BT*

$2,010

1 W UHF transceiver with internal battery. Suitable for TRIUMPH-2 Base or as repeater.

HPT435BT*

$2,710

High power (up to 35 W) UHF transceiver. Suitable for TRIUMPH-1M/TRIUMPH2 Base or as repeater.

Bluetooth antenna

5 STATUS LEDs

2 Buttons

Radio antenna

Bracket

Micro USB connector

JRADIO*

$1,190
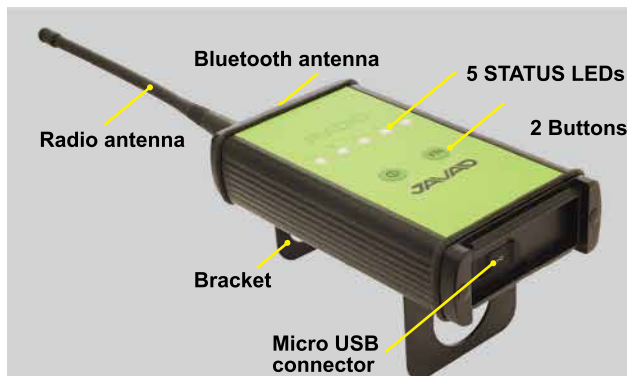
Tri-band UHF receiver with Bluetooth, USB, and internal battery. Suitable for TRIUMPH-2 Rover.

Modems

Multi-point Localization

Useful for relating RTK points to a local system of points with an unknown relationship to the Earth, such as a terrestrial survey. Also it could be leveraged to perform quality control analysis on points used in the localization as well as pitfalls that can occur with using a tilted plane.

I've provided the minimum information needed for the localization to determine a rotated, or tilted, plane. But notice that even C2, L002 is looking pretty good with a delta U of 0.084 without being used as control.

Keys to Success with Localizations:
Set Base in a suitable location, free from visible obstructions to satellites, away from buildings, trees and structures
Use Fixed Solutions ONLY!!! (PPK is OK)
Select Control Points in suitable locations, free from visible obstructions to satellites, with good geometry related to project site
Use Precise, Undisturbed Points
Make sure Control Coordinates are reliable

Localization with high residuals should not be used to determine design coordinates for the reestablishment of missing monuments. If a pair of points is suspected to be the cause of the high residuals, the association between the pair of points can be changed to a Check type of control.

In this case, the parameters are clearly indicating a problem with the vertical solution of the localization. North Inclination and East Inclination are rotations around the North Axis and East Axis.

Instead, it is much wiser to use the proper geodetic scale factor between the underlying grid and ground. To do this, check the box next to scale and select the button.

In addition to residuals quality control as your source of confidence always look at the parameters under Customize.

See full video at www.javad.com

While the Scale factor is based upon a best-fit solution of the localization points, grid distances between points may not match total station distances. To fix that issue, check the box beside Scale and then tap the Grid-to-Ground button. It will automatically calculates the average grid to ground factor of the survey points used in the localization.

Finally it is time to save the results. The localization is complete.

I am on a job now with 143 iron pins found so far. The J-Tip has been awesome for me.

I was out with another local surveyor on this same job last Saturday, and he carried his classic Schoenstedt. There were signals that his detector did not really give a definite reading on, that the J-Tip did. There was also a railroad spike 6 inch deep in the road that the J-Tip missed, and his Schoenstedt did find. When I put the J-Tip over his spot, I only had a 1.8 positive reading, which did drop back to zero when I moved away. When the spike was exposed, the J-Tip reading was 11 while in contact with the spike.

I am also getting good at judging depths before we dig in the road. I am usually within an inch.

John Evers

As for the performance, you can't beat it. However, I want to put out a kudos to the support team from Javad. My LS had a hiccup a couple weeks back. John Evers worked tirelessly into the evening trying to fix it. When it came time to send it in for repair, Michael Glutting sent me his personal LS to keep me going for the few days until the rental unit arrived. THANKS. I don't think you would see that kind of service from any vendor any where.

Bob Farley

I needed it, the LS and the J-tip found it. Another game changer from Javad.

David M. Simolo

Here is an interesting shot. I wanted to shoot the rebar, on the ground. But, post was in the way. I drove a 16d nail, with it's head cut off, (leatherman did that) and used a plumb bob to get it just right. Then, took the LS off the pole, and there is a small hole in the "handle" which I placed over the headless nail. It sat and shot it, while I did other things.
As you can see, by the tree, and shade, this is not a shot for just any GPS.

Nate

SW Arkansas, USA, Planet Earth

Deformation analysis of the Balkan Peninsula from GPS data 2011–2016

The present work is an extended study of the surface movements of the territory of Bulgaria over the territory of the Balkan Peninsula (BP) and mainly of its central and southern part

Keranka Vassileva PhD
Professor, National Institute of Geophysics, Geodesy and Geography, Bulgarian Academy of Science, Bulgaria

Georgi Valev DSc
Professor, Konstantin Preslavsky University of Shumen, Bulgaria

Mila Atanasova–Zlatareva PhD
Assistant Professor, National Institute of Geophysics, Geodesy and Geography, Bulgarian Academy of Science, Bulgaria

The territory of the Balkan Peninsula is well known as a very active tectonic zone. Various geophysical, geological and geodetic methods and approaches have been applied to study and interpret the recent active earth crust movements [2], [6], [7], [9], [10] of the region. The present work is an extended geokinematics study not only for the territory of Bulgaria [13], [14] but it covers the territory of the Balkan Peninsula. Analysis and interpretation of the results obtained is based on the estimated station movements within the time span 2011-2016 from GNSS data processing and application of developed by the authors Finite Elements Method (FEM) for the space [13], [14]. The results of obtained relative deformations have been analyzed and mathematical-geometric interpretation has been performed. Suggested areas of extension (dilatation) and compression have been inferred.

Finite Elements Method (FEM) for the space

For the majority of studies the FEM is mainly used in the analysis of movements of stations, which are results from GNSS data processing in order to be obtained strain tensors and strain accumulation [1], [3], [5], [12]. Since the Balkan Peninsula is relatively large region, the method of finite elements is developed by the authors specifically for the space. More detail theory of the developed method has been presented in [13], [14]. Below only the key points of the theory are given.

The ellipsoidal station coordinates $P(\varphi, \lambda, h)$ obtained from the GNSS data processing are input data used in FEM after stations projecting [10] onto the ellipsoidal surface and their transformation into Cartesian station coordinates $P_0(X_0, Y_0, Z_0)$.

Each station P_0 must satisfy both the equation of meridian ellipse and the equation of the normal line through the station $P (X, Y, Z)$ to this ellipse, namely

$$(1) \quad r_0^{\,2} + Z_0^{\,2}(1+e'^2) = a^2$$

$$(2) \quad \frac{Z - Z_0}{r - r_0} = \frac{Z_0(1 + e'^2)}{r_0},$$

where r_0 is the radius of the parallel, which passes through station P_0 and r is the distance from station P to the Z axis, e' – the second eccentricity of the ellipse. After mathematical operations and modifications finally the Cartesian station coordinates (X_0, Y_0, Z_0) of station P_0 are calculated by

$$(3) \quad X_0 = X\frac{r_0}{r}, Y_0 = Y\frac{r_0}{r}, Z_0 = Z\frac{r_0}{r}.$$

The lengths of the ellipsoidal chords (baselines) $S_{i,k}$ between triangle apexes i and k (i, j, k – triangle apexes) of the finite elements on the ellipsoidal surface are determined from the relationships for the space, i.e.

$$(4) \quad S_{i,k} = \sqrt{(X_k^o - X_i^o)^2 + (Y_k^o - Y_i^o)^2 + (Z_k^o - Z_i^o)^2}.$$

The relative linear deformations m of the triangle sides are obtained from the following equations

(5) $m_{i,j}-1=\dfrac{S'_{i,j}-S_{i,j}}{S_{i,j}}, m_{j,k}-1=\dfrac{S'_{j,k}-S_{j,k}}{S_{j,k}}, m_{k,i}-1=\dfrac{S'_{k,i}-S_{k,i}}{S_{k,i}},$

where S, S' are the lengths of the respective triangle sides at two observation epochs t and t'.

Applying respective relationships [14] between $m_{i,j}$, $m_{j,k}$, $m_{k,i}$, maximal and minimal deformations (a, b) and angle γ between direction α_a of the maximal deformation and direction α of the respective triangle side ($\gamma = \alpha - \alpha_a$), the semi-axes of the ellipses of deformations a, b are obtained from the following equations

(6) $(b^2-a^2)=(m_{j,k}^2-m_{i,j}^2)/(\sin^2\gamma_{j,k}-\sin^2\gamma_{i,j})$,

(7) $a=\sqrt{m_{i,j}^2-(b^2-a^2)\cdot\sin^2\gamma_{i,j}}$

(8) $b=\sqrt{a^2+(b^2-a^2)}.$

Finally the principal relative deformations a' and b' (major and minor) and their directions are determined from

(9) $\begin{aligned}a'&=1-b\\b'&=1-a\\\alpha_b&=\alpha_a+90°.\end{aligned}$

Processing of GNSS observations

The territory of the study is covered by 33 GNSS permanent stations and 11 IGS GNSS permanent stations have been involved for referencing. On a tectonic map after Froizheim et al., 2014 [4], locations of the Balkan Peninsula GNSS stations are shown (Figure 1). Line AA' is a line of cross section of the Hellenides and Rhodope Metamorphic Complex according to [4].

One week data from each year are used from all six years – 2011, 2012, 2013, 2014, 2015 and 2016. The data are processed with Bernese software, Version 5.0 in coordinate system ITRF2008. Obtained normal equations from data processing of each year have been combined in Addneq2 program of the Bernese software. Finally, the estimated station coordinates (X, Y, Z) and station velocity components (V_X, V_Y, V_Z) of all stations have been obtained by applying the least squares method with minimum constraint conditions for coordinates

and velocities of 8 selected reference IGS stations in the system ITRF2008, referred to epoch 2005.0. The root mean squire (*rms*) errors of determined station velocities from data processing in north (V_N) and in east (V_E) components for all stations are 0,1-0,2mm/yr and for vertical component (V_U) -0,2-0,3mm/yr. The estimated station velocity vectors in this study confirm their magnitude and directions obtained in previous investigations of the authors [13], [14], [15].

The relative movements of the stations with respect to the stable part of Europe (ETRF horizontal station velocity vectors in ETRF2000) have been derived from ETRF components of the Eurasia plate rotation pole [15] (*Figure 2*). The obtained horizontal station velocities vary from 0,3mm/yr up to 8,0mm/yr. For three stations (Brai, Alex, Nvrk) the obtained results are not reliable and they are not used in further analysis.

Analysis and discussion of deformations

The final elements (triangles) have been configured approximately as equilateral triangles with approximately equal areas and not overlapping.

16 relatively uniform triangles (Figure 3) have been configured. The ETRF2000 coordinates (X, Y, Z) of all stations in each year have been transformed into ellipsoidal station coordinates (φ, λ, h) and then they have been transformed according to the equation (3) into Cartesian station coordinates (X_0, Y_0, Z_0) onto the ellipsoidal surface used. The (X_0, Y_0, Z_0) station coordinates have been used for determination of the ellipsoidal chords (baselines) between projected stations on the ellipsoidal surface by formula (4). The ellipsoidal chords form the triangle sides of every finite element in each year.

Three main types of deformations have been determined for the time period of five years 2011-2016 by FEM: station displacements, relative side deformations and relative principal deformations.
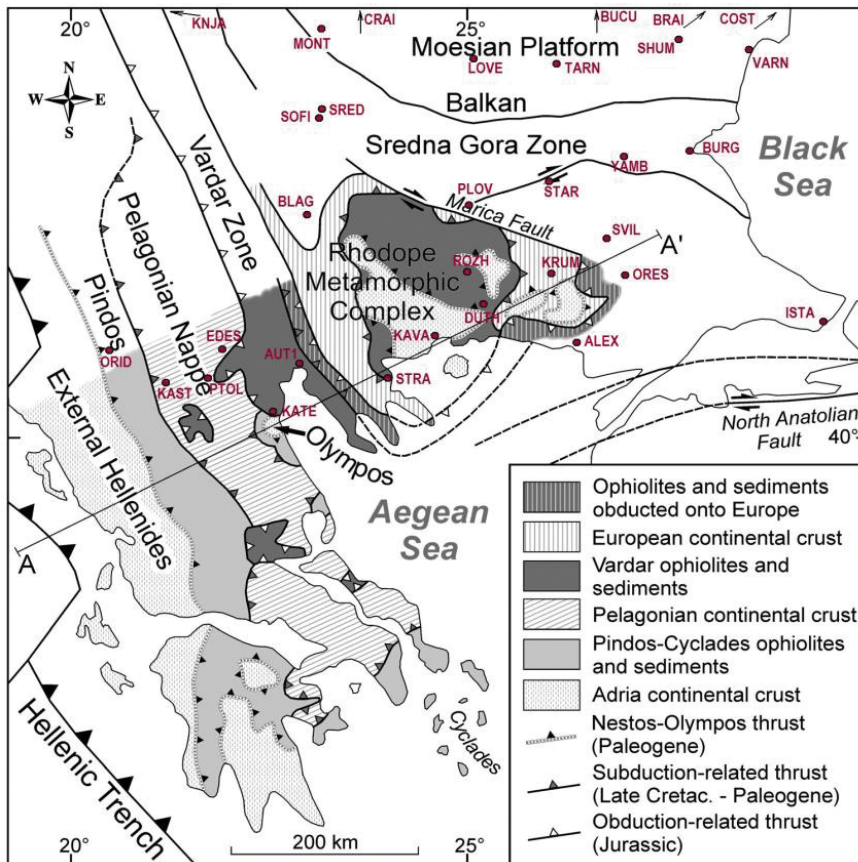

Figure 1. BP GNSS permanent stations involved in this study on the tectonic map of the Balkan Peninsula (after Froitzheim et al. 2014)

Station displacements

Displacements and their directions for each station within the time span 2011-2016 are shown with solid red lines in figure 3. The stations in central and eastern part of the region have moved to the south-west with about 3cm except stations Burg and Ores which movement is small, about 3mm. Stations in the west area – Crai, Knja, Blag, Kava have moved to the south-east as the displacement of the first three stations is 0,5-1,4cm and Kava has moved with 2,5cm. Two of the most southwest stations Orid and Aut1 have moved with 3cm and 5cm respectively to the south-west.

Relative side deformations

Relative deformations of compression (blue) or extension (red) of the triangle sides obtained by formula (5) are shown in figure 3. Small relative side deformations of compression ($0,11.10^{-7}$-$0,49.10^{-7}$, corresponding to 0,11-0,49mm per 10km) have been established for the triangles in the area of Moesia platform. Only the compression of sides Bucu-Crai and Cost-Burg is 1,8mm, respectively 1,6mm per 10 km. Deformations of compression have been also defined by finite elements (Knja, Love, Blag) and (Love, Blag, Plov), which cover the western part of the study region and by the finite element (Blag, Plov, Kava). The relative side deformations obtained are between $0,64.10^{-7}$ and $1,59.10^{-7}$. An area showing relatively compact deformation zone of extension has been inferred by the stations Knja, Blag, Aut1, Kava, Orid in the south-west part. The largest extensions in mentioned area belong to the sides Aut1-Kava ($2,86.10^{-7}$), Blag-Aut1 ($2,42.10^{-7}$) and Orid-Blag ($1,46.10^{-7}$). The relative side deformations along the Black Sea cost and in the most south-eastern area (Burg, Ores, Ista) are also dominantly of compression. It should be noted that according to the developed FEM the type of side deformations (compression or extension) of each finite element depends on the directions of displacements of the respective triangle apexes (stations). The results obtained in this study for station displacements and side deformations of the finite elements (Figure 3) demonstrate a very good agreement.

Relative principle deformations

The relative principal deformations of each finite element are obtained by formula (9) and they are shown in figure 3 (compression in blue and extension in red).

Relative principal deformations of finite elements in the Moesia plate during the time period 2011-2016 are dominantly
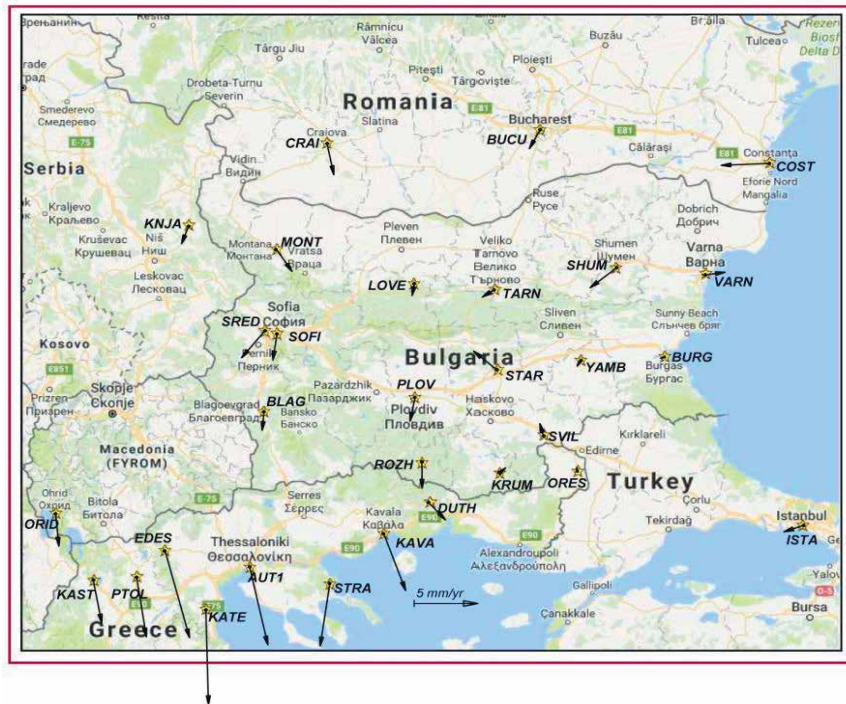

Fig. 2. ETRF2000 horizontal velocity vectors of BP GNSS permanent stations from this study

Figure 3. Relative side and principal deformations and vectors of station displacements for the time span 2011–2016. Relative deformations of 5.10^{-7} correspond to 5mm compression (in blue) or extension (in red) per 10km.

of compression from 0,35mm up to 2,03mm per 10km and directions are mainly northwest-southeast. The relative principal deformations of compression in direction northeast-southwest direction in the north-east area, close to the northern Black Sea coast are approximately the same size as those of their extension (northwest-southeast direction). The results for western part of the study region, closed between the stations Knja, Love, Plov, Kava and Blag and for the most south-east part show deformations of compression in directions southwest-northeast up to west-east and east-west. The extensions in the central-east part and in the central-south part of the region are approximately the same size as the compressions with north-south direction, respectively with southeast-northwest direction. Principal deformations of the most west and south-west part of the Balkans covering the north and northwest Greece, south Macedonia, part of Serbia and western Bulgaria are of extension in all direction. The relationship between directions of the principal deformations of each finite element and the directions of its side deformations is very close. Directions of the principal deformations of extension or compression of every finite element dominantly are defined by the type of deformations of the sides of the respective finite element. The obtained results for the principal deformations in this study confirm this relation (Figure 3).

Conclusion

The finite elements method in space is applied for deformation analysis mostly of the central and southern territory of the Balkan Peninsula for the first time and it is an attempt to be applied another approach in surface geokinematics. The suggested areas of extension and compression and their analysis present a mathematical-geometrical interpretation of the movements of the Balkans region. The results obtained in this study cannot be compared directly to the strain rates results of other studies of the Balkan Peninsula due to the different nature of the approaches.

References

[1] Bogusz, J., A. Klos, M. Figurski, M. Jarosinski, B. Kontny. (2013). Investigation of the reliability of local strain analysis by means of the triangle modelling. Acta Geodyn. Geomater., Vol. 10, No. 3 (171), 293–305.

[2] Burchfiel, B. C., R. W. King, A., Todosov, V., Kotzev, N., Dumurdzanov, T., Serafimovski, B., Nurce. (2006). GPS results for Macedonia and its importance for the tectonics of the Southern Balkan extensional regime, Tectonophysics, 413, 239–248.

[3] Deniz, I., H. Ozener. (2010). Estimation of strain accumulation of densification network in Northern Marmara Region, Turkey. Nat. Hazards Earth Syst. Sci., 10, 2135–2143, www.nat-hazards-earth-syst-sci.net/10/2135/2010

[4] Froitzheim, N., S. Jahn-Awe, D. Frei, A. N. Wainwright, R. Maas, N. Georgiev, T. J. Nagel, J. Pleuger. (2014). Age and composition of meta-ophiolite from the Rhodope Middle Allochthon (Satovcha, Bulgaria): A test for the maximum-allochthony hypothesis of the Hellenides, Tectonics, 32, doi:10. 1002/2014TC003526.

[5] Hu, Y., K. Wang, J. He, J. Klotz, G. Khazaradze. Three-dimensional viscoelastic finite element model for postseismic deformation of the great 1960 Chile earthquake. Journal of geophysical research, 2004, Vol. 109, B12403.

[6] Kotzev, V., R.W. King, B.C. Burchfiel, A. Todosov, B. Nurce, R. Nakov. (2000). Crustal motion and strain accumulation in the South Balkan Region Inferred from GPS Measurements, in Husebye, E., ed., Earthquake monitoring and seismic hazard mitigation in Balkan countries: Proceedings of the NATO Advanced Research Workshop on Earthquake Monitoring and Seismic Hazard Mitigation in Balkan Countries, Borovetz, Bulgaria, 11–18 September 2005: NATO Science Series IV: Earth and Environmental Sciences. Volume 81, 19–43.

[7] Matev, K. (2011). GPS constrains on current tectonics of southwest Bulgaria, northern Greece and Albania. Thesis, Doctor of university of Grenoble, 203 pp.

[8] Milev, G., Dabovski, C. (Eds). (2006). Geodynamics of the Balkan Peninsula, Monograph, Reports on Geodesy, Warsaw University of Technology, Institute of Geodesy and Geodetic Astronomy, 647 pp.

[9] Reilinger, R., S. McClusky, D. Paradissis, S. Ergintav, Ph. Vernant. (2010). Geodetic constraints on the tectonic evolution of the Aegean region and strain accumulation along the Hellenic subduction zone. Tectonophysics, 488, 22–30.

[10] Stangl, G., Ph. Mitterschiffthaler. (2015). A GNSS-derived Velocity Field of the Southern Balkan Peninsula. Geophysical Research Abstracts, 2015, Vol. 17, EGU2015-8362, EGU General Assembly 2015.

[11] Valev, G. (1987). Projection of points onto the earth ellipsoid. Geodesy, Cartography and Land Management, 4, 6-11. (in bulg.)

[12] Valev, G., P. Kastreva. (2006). Stress strain analysis of the Balkan Peninsula. Balkan Peninsula monograph, Reports on Geodesy, Warsaw University of Technology, No 5(80), 597-605.

[13] Vassileva, K., G. Valev (2015). Application of Finite Elements Method in space for deformation analysis of the territory of Bulgaria, Proceedings of the 8-th Congress of the Balkan Geophysical Society, 4-8 October, Crete, Chania, Greece, 5p. art. N. 26716.

[14] Vassileva, K., G. Valev. (2015). Deformation analysis of the Territory of Bulgaria from GNSS observations. Coordinates, Vol. XI, Issue 12, 12-15.

[15] Vassileva, K., Atanasova, M. (2016). Earth movements on the territory of Bulgaria and northern Greece from GPS observations. Comptes rendus de l'Académie bulgare des Sciences, Volume 69, Issue 11, 1473-1478.

[16] http://epncb.oma.be/_ productsservices/coord_trans/

[17] ftp://olggps.oeaw.ac.at/ CEGRN15/solutions

UAS in India: From a 'no fly zone' to a 'fly zone'

The Directorate General of Civil Aviation (DGCA) announced draft regulations / civil aviation requirements (CARs) on civil use of Remotely Piloted Aircraft Systems (RPAS), commonly known as drones on November 1, 2017. Readers may go through the draft and comment

The Union Minister of Civil Aviation Shri P. Ashok Gajapathi Raju and the Minister for State for Civil Aviation Shri Jayant Sinha presented and briefed the media about the draft regulation. The draft is open for discussion and people can share their feedback with DGCA by December 1, 2017.

This is an encouraging development as uses of drones are banned since October 2014 by the DGCA primarily due to security issues. In April 2016, DGCA came out with draft guidelines to regulate the civilian uses of UAVs but somehow the same was not finalized.

The draft starts with defining the Unmanned Aircraft System (UAS) that's consists of an Unmanned Aircraft (UA), a Remote Pilot Station (RPS), Command and Control (C2) Link, the maintenance system and the operating personnel. Remotely Piloted Aircraft (RPA), autonomous aircraft and model aircraft are various sub-sets of UAS.

If further states that UAS operations present problems to the regulator in terms of ensuring safety of other users of airspace and persons on the ground. However, in view of technological advancements in UAS over the years and their increased civil applications, it has become necessary to develop regulations for operations of this activity.

Categories

The draft classifies Civil RPA in accordance with Maximum Take-off Weight (MTWO) as mentioned in Table 1.

Table 1: Civil RPA classification in accordance with Maximum Take-off Weight (MTWO)

1	Nano	Less than or equal to 250 gm
2	Micro	Greater than 250 gm and less than or equal to 2 kg
3	Mini	Greater than 2 kg and less than or equal to 25 kg
4	Small	Greater than 25 kg and less than or equal to 150 kg
5	Large	Greater than 150 kg

Requirement of Unique Identification Number (UIN)

All civil RPA shall require to obtain Unique Identification Number (UIN) from DGCA. The exceptions are RPA in Nano category with an intent to fly upto 50 ft AGL, and those owned & operated by Government security agencies are exempted from obtaining UIN.

Eligibility for UIN

UIN will be granted where the RPAS is wholly owned either:
a) By a citizen of India; or
b) By the Central Government or any State Government or any company or corporation owned or controlled by either of the said Governments; or
c) By a company or a body corporate provided that:
   i) it is registered and has its principal place of business within India;
   ii) its chairman and at least two-thirds of its directors are citizens of India; and,
   iii) its substantial ownership and effective control is vested in Indian nationals; or
d) By a company or corporation registered elsewhere than in India, provided that such company or corporation has leased the RPAS to any organization mentioned in b and c above.

Required documents

Along with the contact details of operator (with valid proof), the applicant should mention the purpose and area of operation, specification of RPAS and the details of compatible payload (with its weight and maximum weight carrying capacity of the RPAS). Copy of RPA Flight Manual/ Manufacturers Operating Manual and Copy of Manufacturer's maintenance guidelines for RPA will also be required.

Clearances
- Permission for all frequencies used in RPA operations from Department of Telecommunication (Wireless Planning and Coordination Wing);
- Security Clearance from MHA (except those owned and operated by Government security agencies)
- Verification of character and antecedents of the remote pilot(s) from local sub-divisional police office.

The identification plate (made of fire proof material) inscribed with UIN, RF ID tag and SIM shall be affixed to the RPA.

Requirements for Issue of Unmanned Aircraft Operator Permit (UAOP)

All civil RPA operations for any purpose whatsoever will require UAOP from DGCA.

However, following are exempted for UAOP

a) Nano RPA operating below 50 ft AGL in uncontrolled airspace & indoor operations.

b) Micro RPA operating below 200 ft AGL in uncontrolled airspace and clear of prohibited; restricted and danger areas; Temporary Segregated Areas (TSA) and Temporary Reserved Areas (TRA) as notified by AAI in the AIP. However, the user shall intimate the local police authorities before conduct of actual operations.

c) RPA owned and operated by Government security agencies. However, the agency shall intimate local police authorities and concerned ATS Units before conduct of actual operations.

All civil RPA operators shall submit duly filled application along with requisite fees as per Rule 15A of Aircraft Rules 1937 for issue of UAOP to DGCA at least 7 days prior to actual conduct of operations along with following documents:

a) Permission from ATS provider (civil/defense);

b) Permission of the land/property owner (area used for take-off and landing of RPA);

c) Details of remote pilot(s) and training records;

d) Insurance details (as applicable);

e) Security programme as approved by BCAS.

The UAOP shall be issued by DGCA as per the format given at Annexure-VI with a copy to MHA, BCAS, IAF, ATS Provider (AAI/MoD), and district administration (Superintendent of Police) for information.

Validity of the UAOP shall be for a period of five years from the date of issue. Renewal of the UAOP shall be subject to fresh security clearance from MHA. UAOP issued by DGCA shall be non-transferrable.

DGCA may impose additional requirements depending upon justification on case- to-case basis.

Security/safety aspect

The owner/operator shall be responsible for the safe

General Requirements

Item/ Category	Nano (≤250 gm)	Micro (>250gm≤2kg)	Mini & Above (>2kg≤25kg) (>25kg≤150kg) (>150kg)	Model Aircraft, MTOW < 2kg
Security clearance (organisation)	✖	✔	✔	✖
Unique Identification No. (UIN)	✖	✔	✔	✖
Unmanned Aircraft Operator Permit (UAOP)	✖	✖	✔	✖
Remote pilot approval requirement	✖	✖	✔	✖
Approval Time for UIN/UAOP	✖	02 days	02/07 days	✖

Operational Requirements

Item/ Category	Nano (<250 gm)	Micro (>250gm<2kg)	Mini & Above (>2kg<25kg) (>25kg<150kg)(>150kg)	Model Aircraft, MTOW < 2kg
Height Allowed (AGL)	50 ft	200 ft	200 ft (>200 ft restrictive)	200 ft
VLoS and Day Operations	✔	✔	✔	✔
Flight Plan	✖	✖	✔	✖
ADC/ FIC	✖	✖	✔	✖
Local Police	✖	✔	✔	✔
Area of Operation	Uncontrolled airspace and indoor	Uncontrolled airspace	Controlled and uncontrolled airspace	Educational institution premises

Mandatory Equipment Requirements

Item/ Category	Nano (<250 gm)	Micro (>250gm<2kg)	Mini & Above (>2kg<25kg) (>25kg<150kg) (>150kg)	Model Aircraft, MTOW < 2kg
ID Plate	✖	✔	✔	✔
RF ID/ SIM	✖	✔	✔	✖
GPS	✖	✔	✔	✖
RTH (Return to Home)	✖	✔	✔	✖
Anti Collision Light	✖	✔	✔	✖

<u>Note</u>: For Govt. Security Agencies, no approval required except intimation to Local Police and ATC before operation

Source: http://pibphoto.nic.in/documents/rlink/2017/ nov/p201711201.pdf Image source.

custody, security and access control of the RPAS. In case of loss of RPA, the operator shall report immediately to local administration/police, BCAS and DGCA.

The RPAS operator shall ensure that all security measures as enumerated in the Security Programme (approved by BCAS) are in place before operation of each flight.

The ground control station (while in use or in store) shall be secured from sabotage or unlawful interference.

The owner/operator of all RPA except Nano RPA shall be responsible for notifying any incident/accident involving RPA to the Director of Air Safety, DGCA who will further intimate to all the concerned agencies.

The RPAS (issued with UIN) shall not be sold or disposed-off in any way to any person or firm without permission from DGCA. In case, the RPA is damaged and cannot be restored to original condition, the same shall be intimated to DGCA by owner/operator for cancellation of UIN.

Training requirements for remote pilots

Remote pilot shall have attained 18 years of age with thorough ground training equivalent to that undertaken by aircrew of manned aircraft or a PPL holder (Aeroplanes/Helicopter) with FRTOL.

Remote pilots shall undergo thorough practical training on the control of a RPA in flight, which may consist of a proportion of simulated flight training.

The training shall include the following:
    a) Basic Radio Telephony (RT) techniques including knowledge of radio frequencies.
    b) Flight Planning and ATC procedures.
    c) Regulations specific to area of operations.
    d) Basic knowledge of multi rotors and fixed wing operations.
    e) No-fly zone awareness.

The training shall enable the remote pilot to demonstrate that he/she can control the RPA throughout its operating conditions, including safe recovery during emergencies and system malfunction.

The training requirements are not applicable for Nano and Micro category RPA. However, the user shall be fully aware of his/her responsibilities to fly these machines safely.

RPAS Maintenance

Maintenance and repair of RPAS shall be carried out in accordance with the manufacturer s approved procedures, as applicable.

Maintenance of the ground control equipment shall be carried out in accordance with the manufacturer s recommended inspection and overhaul interval, as applicable.

The remote pilot/user shall not fly the RPA unless he/she is reasonably satisfied that all the control systems of RPA including the radio link are in working condition before the flight.

The UAOP holder shall maintain records (till the RPAS is in service) of each RPA flight and make such records available to the DGCA on demand.

Equipment requirements

All RPA except Nano shall be equipped with the following serviceable components/ equipment:
    a) Identification Plate
    b) GPS for horizontal and vertical position fixing
    c) Autonomous Flight Termination System or Return to Home (RH) option
    d) Flashing anti-collision strobe lights
    e) RFID and GSM SIM Card Slot for APP based tracking

The RPA intending to operate at or above 200 ft AGL shall carry the following equipment/capabilities in addition to

those specified above of this CAR:
    a) SSR transponder (Mode C or S) or ADS-B OUT equipment
    b) Barometric equipment with capability for remote subscale setting
    c) Geo Fencing capability
    d) Detect and Avoid capability

Remote pilot shall be equipped with communication facilities to establish and maintain continuous two-way communication with the concerned ATS unit.

The GPS tracking system of the RPA shall be self-powered and tamper/ spoofing proof to ensure data relay even in the event of RPA accident.

Airports Authority of India and Indian Air Force shall monitor RPA movements in the country.

Requirements for operation of RPA

The RPA operator shall prepare SOP, which shall contain following procedures according to the provisions contained in relevant sections of AIP-India:
    a) Take-off/landing
    b) Collision avoidance
    c) Noise abatement
    d) Flight plan filing
    e) Local airspace restriction
    f) Right-of-way
    g) Communications
    h) RPA emergency including loss of C2 link

i) Safe recovery of RPA through controlled airspace in case RPA system failure precludes the ability to remain outside controlled airspace, etc.

Nano and Micro RPA while operating upto 50 ft and 200 ft AGL respectively are exempted from filing the flight plan and obtaining ADC.

Irrespective of height, operation of RPA in Mini and above category shall be conducted only after filing flight plan and obtaining following clearances:

a) Nearest ATC Unit
b) Air Defence Clearance (ADC)
c) Flight Information Centre (FIC)

All RPA operator except Nano RPA shall inform the concerned local police authority in writing prior to commencing the operations.

In the event of cancellation of operations, the operator shall notify the same to all appropriate authorities immediately.

Irrespective of weight category, all RPA operations are restricted to day operation and within Visual Line of Sight only.

RPA shall be operated only when the following meteorological conditions exist:
a) During daylight (between sunrise and sunset).
b) In Visual Meteorological Conditions (VMC) with a minimum ground visibility of 5 km and cloud ceiling not less than 450 m (1500 ft).

c) Surface winds of not more than 10 knots.
d) No precipitation (rain, hail or snow) or thunderstorm activities.

Remote pilots shall prefix RPA call-sign with the word UNMANNED during voice communications between ATC and the remote pilot station. RPA operator shall ensure that no Radio Frequency Interference (RFI) is caused to air traffic operations and air navigation equipment.

For intended operations of RPA in controlled airspace, the remote pilot shall establish contact with ATC prior to entering the controlled airspace.

RPA Operator shall carry out safety assessment of the RPA operations including that of launch/recovery sites. The site (including emergency operation zone and any safety zone for the operations of the RPAS) shall be under the full control of the operator.

The take-off and landing areas should be properly segregated from public access.

Designated safe areas should be established by the RPA Operator for emergency RPA holding and flight terminations.

No person shall act as a remote pilot for more than one unmanned aircraft operation at a time.

If two or more persons are available as remote pilots for a flight, at any given moment, there shall be only one person acting as a remote pilot-in-command.

RPA Operator shall be responsible for ensuring that the RPA is operated safely and remains clear of all manned/unmanned air traffic, terrain and obstacles.

RPA shall, at all times, give way to manned aircraft. 12.17 RPA shall not be flown in

RPA shall not discharge or drop

substances unless specially cleared and mentioned in UAOP.

RPA shall not transport any hazardous material such as explosives or animal or human payload.

RPA operator/remote pilot shall be liable to ensure that privacy norms of individuals are not compromised in any manner.

The CRA lists the no drone zone areas (Table)

Legal obligations

13.1 UIN and/or UAOP issued by DGCA shall not:
   a) Confer on RPAS operator any right against the owner or resident of any land or building or over which the operations are conducted, or prejudice in any way the rights and remedies which a person may have in respect of any injury to persons or damage to property caused directly or indirectly by the RPA.
   b) Absolve the operator/remote pilot from compliance with any other regulatory requirement, which may exist under the State or local law.

Insurance

All civil RPAS operators shall have insurance with the liability that they might incur for any damage to third party resulting from the accident/incident.

To encourage new technology, Indian organisations involved in R & D related activity of RPAS, having obtained industrial license from DIPP, shall use the test sites indicated in Annexure-VIII for testing/demonstration purpose.

No drone zone
- Within an area of 5 km (2.7 NM) from Aerodrome Reference Point of operational airports;
- Above the Obstacle Limitation Surfaces (OLS) of an operational aerodrome specified in Ministry of Civil Aviation (Height Restrictions for Safeguarding of Aircraft Operations) Rules, 2015 notified through Gazette of India notification GSR751(E) or its amendments;
- Within permanent or temporary Prohibited, Restricted and Danger Areas including TRA and TSA as notified by AAI in AIP;
- Without prior approval, over densely populated areas or over or near an area affecting public safety or where emergency operations are underway;
- Within 50 km from international border which includes Line of Control (LoC), Line of Actual Control (LAC) and Actual Ground Position Line (AGPL);
- Beyond 500 m (horizontal) into sea from coast line provided the location of ground station is on fixed platform over land;
- Within 5 km radius from Vijay Chowk in Delhi;
- Within 500 m from perimeter of strategic locations notified by Ministry of Home Affairs;
- Within 500 m from perimeter of military installations/ facilities;
- From a mobile platform such as a moving vehicle, ship or aircraft; and
- As an autonomous flight, unless it is following an Autonomous Flight Termination (AFT) or Return to Home (RH) procedure.
- Over eco-sensitive zones around National Parks and Wildlife Sanctuaries notified by Ministry of Environment, Forests and Climate Change without prior permission.

List of identified area for testing/demonstration of UAS

State	Name of Place
Punjab	Phagwara
Uttarakhand	Sakkhanpur Farm
Uttar Pradesh	Lucknow, Shivgarh Resorta
Uttar Pradesh	Sultanpur
Karnataka	Chitradurga
Karnataka	Ganimangala Village
Kerala	Munnar,Devikulam
Kerala	Idukki
Tamil Nadu	Vellore
Tamil Nadu	Coorg, Choudigudi Estate
Tamil Nadu	Salem, Pullagoundanpatti
Tamil Nadu	Erode, Nambiyur
Tamil Nadu	Coimbatore, Chettipalayam
Telangana	Hyderabad, Mulugu Village
Assam	Sonapur, Betkuchi
Assam	Sivasagar
Arunachal Pradesh	Daporijo Airfield
Gujarat	Surendranagar
Maharashtra	Shirpur Airport
Maharashtra	Amravati
Maharashtra	Aurangabad
Maharashtra	Ahmednagar
Maharashtra	Satara

The above list of Identified Area for Operation of UAS excludes the restricted areas notified by various Government agencies.

It is the responsibility of such Indian operators to ensure that UAS manufacturers to ensure that no manned or unmanned aircraft is flying during the intended timeframe in the intended test area.

For detailed draft, visit http://www.dgca.nic.in/misc/draft%20 cars/CAR%20-%20UAS%20(Draft_Nov2017).pdf

3D Australia 2017 report

The inaugural 3D Australia conference was at the University of Melbourne from 24th to 27th October 2017. 3D Australia 2017 comprised the 3D Geoinfo Conference 2017, the 1st international workshop on BIM and GIS integration, and 3D Cadastre training.

The 3D Geoinfo Conference 2017 brought together 150 international researchers from

academia, industry and government in the field of 3D spatial information. It provided an interdisciplinary forum in the fields of data collection, advanced modelling approaches, data analysis and visualisation.

The attendees enjoyed excellent keynote lectures on topics related to the national approach for 3D SDIs, nD systems for cities, the changing role of surveyors and spatial professions driven by 3D technologies, cultural shift to achieve smart cities and the role of standards in nD city systems.

There were 43 scientific papers submitted to the conference. After the double-blind peer review process, 16 papers were accepted and published in ISPRS Annals (Volume IV-4/W5) and eight papers in ISPRS archives (Volume XLII-4/W7) both available online as open access proceedings. The papers covered a range of topics related to 3D geospatial data including drivers of 3D data, reasoning and structuring 3D data, 3D indoor data, several applications of 3D data such as energy analysis, asset management,

cadastres and much more. The papers also included some examples of how 3D data is being used by public sector agencies. There were many promising future research presented as short papers.

BIM-GIS Integration was a pre-conference workshop session of 3D GeoInfo 2017 organised by the BIM Working Group of the International Association of

Geodesy. The workshop provided a platform for researchers to present and discuss their work in various aspects of BIM and GIS integration. The focus of the workshop was on the nexus of BIM and GIS to discuss the challenges of integrating BIM and GIS. There were ten papers presented during the workshop through which several challenges were identified including leadership, advocacy, collaboration inter-domain and intera-domain, best practices, funding models for BIM and GIS integration, BIM and City Models data value and IP, standards and scales, BIM to 3D GIS workflow, data models based on concepts and ontologies, cross-domain curriculum development and BIM/GIS issues in the context of current social constructs (public and private sectors).

There was also a recognition of cross-domain collaboration in this space such as those between OGC, buildingSmart and ISO. The need for academic community input more into BIM and GIS standards was strongly highlighted.

The 3D Cadastre training presented the Centre for Spatial Data Infrastructures and Land Administration's previous and current research topics related to 3D Cadastre. It also provided training on the implementation of 3D digital cadastral systems. There were 40 attendees all of which received a certificate of attendance from the Centre for Spatial Data Infrastructure and Land administration, the University of Melbourne.

The attendees enjoyed the Australian hospitality including Melbourne famous coffee, international food, Aussie BBQ and Australian Aboriginal music.

The conference presentations are now available at http://3dgeoinfo2017.com.

Mohsen Kalantari and Abbas Rajabifard, University of Melbourne, Australia.

Galileo update

No UK firms for European space contracts due to Brexit uncertainty

British firms are being "excluded" from bidding for lucrative space contracts due to concerns over Brexit. Simon Henley, the president-elect of the Royal Aeronautical Society, told MPs companies have said they are losing out.

He gave the example of the Galileo programme, Europe's GNSS system, created through the European Space Agency and the European Global Navigation Satellite Systems Agency. UK firms had been "very successful up to date" with regards to work on it, he said.

"But we have had companies now reporting to us that they are being excluded from bidding for contracts on Galileo," he told the Business, Energy and Industrial Strategy Committee for a discussion of Brexit implications for the aerospace industry.

"Although membership of the European Space Agency is not part of the EU discussions, because it's not an EU body, many of the contracts, including Galileo are EU funded," he added. *www.cityam.com*

Galileo satellites readied for December launch

Europe's next four Galileo navigation satellites and the Ariane 5 rocket due to lift them into orbit are being readied for their Dec. 12 launch from Europe's Spaceport in Kourou, French Guiana.

On Nov. 21, Galileo satellites 19–22

were declared ready for flight, along with their Ariane. Combined activities are now under way, culminating in the satellites meeting their rocket in the Final Assembly Building.

The satellites were flown in pairs to French Guiana last month. Once safely unboxed in the Spaceport's cleanroom environment, they were tested to ensure they had suffered no damage during their transatlantic flights.

Next came their fit check, when they were mechanically and electrically linked one by one to the dispenser that will carry them during their ascent to the target 23,500 km-altitude orbit, before releasing them into space.

Last Friday saw the satellites filled with enough fuel to fine-tune their orbits and orientation during their projected 12-year working lives. Next, they will be attached to their dispenser together for the final time.

In parallel, their customised Ariane 5 is being assembled. Two solid-propellant boosters were mated with its main cryogenic stage before the addition of the interstage that carries the electronics to control the vehicle.

Next came the addition of the storable propellant stage, powered by a reignitable engine, which will deliver the quartet to their target orbit.

Once fully checked, the Ariane will be moved to the final building for the addition of the satellites atop their dispenser, sealed within their protective fairing. ◣

3D Laser Mapping campaigns for open-source lidar data

3D Laser Mapping will be offering open access to point cloud data which can be viewed and manipulated using GIS software. This information can be extracted for use by businesses, academic research and for in-house training opportunities.

The company will be releasing data collected using its flexible ROBIN mobile mapping system, which can be used on foot, in a vehicle and mounted to aircraft and UAVs. *www.3dlasermapping.com.*

China successfully launches remote sensing satellites

China has successfully launched remote sensing satellites designed to conduct electromagnetic probes and other experiments.

The satellites, whose number is not specified yet, were launched on a Long March-2C rocket from Xichang Satellite Launch Center in southwestern Sichuan province Xinhua news agency reported. The satellites have entered the preset orbit and the launching mission was proclaimed a success, the report said. *http://economictimes.indiatimes.com*

ISRO to launch remote sensing Cartosat II satellite in Dec

Indian Space Research Organisation has scheduled the launch of Cartosat II remote sensing satellite in the second half of December. The PSLV launch vehicle will carry the satellite along with 28 other foreign satellites and three Indian satellites on commercial basis. According to the Chairman of ISRO, A S Kiran Kumar, ISRO is working towards improving the robustness of PSLV to withstand external variables. *www.ddinews.gov.in*

SimActive automates direct georeferencing

SimActive Inc. has announced an automated solution for direct georeferencing from real-time kinematic (RTK) positioning. Within the new

workflow feature, users can easily get high accuracy in projects without the use of ground control points (GCP), saving considerable time in collecting and processing data. *www.simactive.com.*

DigitalGlobe and Orbital Insight partnership

DigitalGlobe has announced a multi-year agreement with Orbital Insight to expand the scope of their existing data partnership and fuel global-scale analytic solutions.

Orbital Insight, a leader in geospatial analytics, will operate at petabyte-scale as a DigitalGlobe Geospatial Big Data (GBDX) platform partner. With broader access to DigitalGlobe's vast imagery archive, Orbital Insight will further refine its analytic capabilities, which include cases like estimating harvest yields, making more accurate retail predictions, assessing the societal and economic status of large regions and monitoring global energy and natural resource markets.

UAE Space Agency to cooperate with German Aerospace Centre

The UAE Space Agency has signed a memorandum of understanding (MoU) with the German Aerospace Centre, which defines a framework for collaboration and the exchange of information and expertise in the fields of space science, research, technology, and regulation. *http://gulfnews.com*

Velodyne releases VLS–128 Lidar

Velodyne has recently announced its latest product, the VLS-128 which is the most powerful LiDAR developed by it so far. It is capable of providing twice the range and three times the resolution of its predecessor. "This product was designed and built for the level 5, fully autonomous, mobility as a service market," says Anand Gopalan, the company's CTO, meaning it can perform as well or better than a human under any circumstances. ◣

Air Force accepts delivery of GPS Next Generation Operational Control System

The Space and Missile Systems Center announced that the United States Air Force has accepted delivery of the Global Positioning System Next Generation Operational Control System (GPS OCX) Launch and Checkout System (LCS) baseline from Raytheon Intelligence and Information Systems.

Also known as Block 0, LCS demonstrated conformance through test and analysis with all contractual requirements. OCX has had numerous challenges delaying the delivery of this critical capability, and this delivery marks a significant program milestone providing the Air Force with a cyber-hardened ground system to support the launch and on-orbit checkout of the GPS III satellites. OCX Block 0 is the foundation for Raytheon's future Block 1 and 2 delivery, slated for delivery in 2022. *www.losangeles.af.mil*
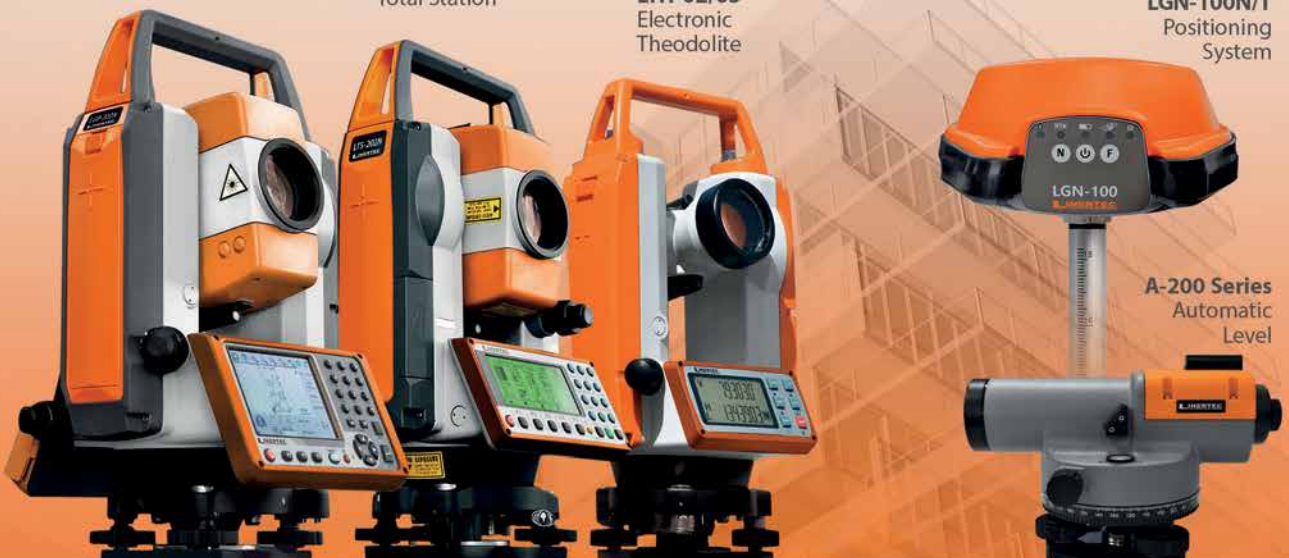
DoT in India exempts feature phones from GPS installation diktat

The telecom department has exempted feature phone makers from installing GPS which helps track the location of a device. The Department of Telecommunications(DoT), which said in April last year that all mobile phones must have GPS capability, has now scaled down the mandate and made it applicable to only smartphones, according to a notification in November.

Almost 400 million people in India still use feature phones and the segment has been aided largely by Reliance Jio Infocomm's 4G Volte feature phone, which then prompted Indian competitors to follow suit and launch their own versions. A recent study by Mobile Marketing Association and Kantar IMRB suggests that 85% of feature phone consumers do not wish to upgrade to smartphones. It remains to be seen whether the government will mandate other tracking tools in feature phones. www.*economictimes.indiatimes.com*

Russia vows to support the Philippines transport development

Transportation Secretary Arthur P. Tugade, Philipines and Russian Minister of Transportation Minister Maksim Sokolov agreed to cooperate on rail, maritime, road and aviation development in the Philippines. The two countries agreed on cooperating for the development of new technologies for road safety. On satellite navigation technologies, the Philippines and Russia will explore utilization of Glonass–similar to GPS– for road-emergency response, truck-weight monitoring and air-navigation applications. *https://businessmirror.com*

Beidou joins global rescue data network

China's domestically developed navigation satellite system Beidou has been included in a global network that collects and distributes data for search and rescue missions, the Ministry of Transport said. Beidou will be part of the International Cospas-Sarsat Programme, a nonprofit, intergovernmental and humanitarian cooperative with 44 members, including the United States, Canada, Russia and China.

The International Cospas-Sarsat Programme is a satellite-based search and rescue distress alert detection and information distribution system best known for detecting and locating emergency beacons activated by aircraft, ships and hikers in distress. It aims to "provide accurate, timely and reliable distress alerts and location data to help search and rescue authorities assist people in distress". It uses the GPS, GLONASS and Galileo systems for its missions.*http://english.cctv.com*

China adds 2 satellites to Beidou

China has added two satellites to its Beidou network. The pair of Beidou-3 satellites were launched aboard a single Long March-3B rocket from the Xichang launch center in the southwestern province of Sichuan, broadcaster CCTV and the Xinhua News Agency reported.

China plans to complete a network linking more than 30 satellites providing real-time geospatial information worldwide by 2020. *www.wsbtv.com*

Australia launches regional SBAS positioning trial

The Federal Government has announced a two-year trial of a new Satellite-Based Augmentation System (SBAS) for the Australasian region recently supported by an investment of $12 million in federal funds, and a further $2 million from the New Zealand government.

The trial will be the first in the world to test the Precise Point Positioning (PPP) technique's integration in an SBAS service, and will be managed by the Australia and New Zealand CRC for Spatial Information (CRCSI), in partnership with satellite communications company Inmarsat, technology firm GMV and security giant Lockheed Martin. Land Information New Zealand (LINZ), the government department responsible for mapping landscapes and charting New Zealand waters, will oversee the New Zealand's involvement in the project.

Businesses and organisations from ten industry sectors including agriculture, aviation, construction, consumer, maritime, rail, road, resources, spatial and utilities will also participate, with over 30 specific projects anticipated. The trial is intended to test the performance of the technology directly across industries; current industry-specific requirements and how they interact with the technology, and future industry-specific innovations that may leverage the technology. The outcome of the trial will in part determine if Australia and New Zealand should develop an operational SBAS.

SBAS is a form of GNSS augmentation — techniques to extend and improve the accuracy, reliability or availability of GNSS systems. SBAS systems use additional satellite-broadcast messages, typically utilising ground stations at surveyed points to record measurements from GNSS satellites, their signals and environmental factors that could impact them. Messages containing these data are created from these measurements that are sent to the SBAS satellites, and then broadcast to end users to improve GNSS capabilities. *www.spatialsource.com.au*

Indian Railways to use GPS–enabled fog safety devices

The Indian Railways has planned to use GPS-enabled fog safety devices in the trains to alert the loco pilot about approaching signals. The GPS-based devices in trains would provide advance warning to motormen and it in next few days all trains will be equipped with it.

The Indian Railways said in a statement that 900 of these GPS devices have been given to the Delhi zone. Besides this, the Railways will also deploy fogmen to place detonators on the tracks to alert the loco pilots about approaching signals. *www.india.com/*

Lockheed Martin assembles third US Air Force GPS III satellite

The U.S. Air Force's third GPS III satellite undergoing production at Lockheed Martin advanced satellite manufacturing facility has been successfully integrated into a complete space vehicle.

GPS III Space Vehicle 03 (GPS III SV03) comes after the first two GPS III satellites on a streamlined assembly and test production line. GPS III SV03 was assembled in Lockheed Martin's GPS III Processing Facility, a $128 million factory designed in a virtual reality environment to boost efficiency and slash costs in satellite production. Now fully assembled, the third satellite is being prepared for environmental testing.

GPS III SV03 closely follows the company's second satellite in the production flow. GPS III SV02 completed integration in May, finished acoustic testing in July and moved into thermal vacuum testing in August. The second GPS III satellite is expected to be delivered to the U.S. Air Force in 2018.

The fourth GPS III satellite is close behind the third. Lockheed Martin received the navigation payload for GPS III SV04 in October and the payload is now integrated with the space vehicle. The satellite is expected to be integrated into a complete space vehicle in January 2018.

In August, Lockheed Martin technicians began major assembly work on GPS III SV05. All of these satellites are following Lockheed Martin's first GPS III satellite, GPS III SV01, through production flow. Lockheed Martin is under contract for ten next generation GPS III satellites as part of the US Air Force's modernized Global Positioning System. GPS III will have three times better accuracy and up to eight times improved anti-jamming capabilities. Spacecraft life will extend to 15 years, which is 25 percent more than the latest GPS satellites on-orbit today. GPS III's new L1C civil signal also will make it the first GPS satellite to be concurrently operable with other international global navigation satellite systems. ◥

EarthSense releases map of air pollution in UK

EarthSense Systems has published MappAir – the first ever high resolution nationwide map of air pollution. Combining data from satellites and its own air quality monitoring sensors together with open source data, it has used complex modelling techniques to create the highly accurate map.

Initially available for the whole of the UK at 100 metre resolution, MappAir shows how air pollution, specifically nitrogen dioxide, changes across the country and within towns and cities, highlighting likely sources and potential clean-air refuge areas. Using the British National Grid, EarthSense has divided the UK into 100 metre squares – about twice the size of an average football pitch.

Air pollution readings from satellites and its own Zephyr air quality monitoring sensors were combined with open data, including traffic emissions and weather conditions, to produce an annual average for each cell. www.earthsense.co.uk

Global Mapper SDK available on Amazon Web Services

Blue Marble Geographics has announced that the Global Mapper SDK has been expanded to provide data processing capabilities in the cloud. Using Amazon Web Services (AWS), developers can utilize Global Mapper's scripting language to provide a range of online data access, creation, editing, conversion, and distribution services for clients and customers by accessing an AWS hosted version of the SDK. www.bluemarblegeo.com

Pitney Bowes launches Global Collaboration Community

Pitney Bowes Inc. has announced the global availability of the Li360 Community, an online community for clients, product engineers, partners and the "GIS curious" to explore

Location Intelligence capabilities, applications and tools to resolve challenges in the market. The Li360 Community is a home for all subject matter experts, and those interested in GIS to generate mindshare that will grow the Location Intelligence market and foster leading innovation.

To date, over 1000 people are accessing the Community to share best practices, analyze case studies, participate in real-time discussions, and identify development needs for Location Intelligence solutions. The Community has received 40,000 page views, and over 15,000 https://li360.pitneybowes.com

ISRO plan to cut down jumbo track deaths

A team from the Kolkatta office of the Indian Space Research Organisation (Isro) visited the Jalpaiguri Government Engineering College to discuss on a prospective project to prevent deaths of elephants on the Dooars rail tracks and help in the forecast and rescue of people during natural calamities in north Bengal though the Geographical Information System.

The organisation is also planning to set up a regional GIS centre at the college, sources said. G Srinivasa Rao, a scientist posted at the Regional Remote Sensing Centre of Isro in Kolkatta said,

"We want to use GIS technology to prevent deaths of elephants and during natural disasters in north Bengal. We had some discussions today and will again visit the college next month."

Russia offers UAE to use its Glonass navigation technologies

Russia is offering the United Arab Emirates (UAE) to use Russian Glonass navigation technologies, the press service of the Russian ministry of industry and trade said after Minister Denis Manturov's talks with Abu Dhabi Crown Prince Mohammed bin Zayed Al Nahyan. ◥

Autonomous flight of "Smart Drone"

Terra Drone Co., Ltd., a leading Japanese industrial drone service provider, and KDDI Corporation, a Japanese telecommunications operator succeeded in a fully autonomous flight experiment of "Smart Drone" using "3D map" and "Drone Port." As a result of the experiment, the world's first long-distance drone flight of about 6.3 km via the "Drone Port" which enables a drone to recharge automatically, successfully returned to the landing site after spraying terraced ponds of Nishikigoi(carp) with pesticide.

This demonstration is an experiment for safe flight altitude setting on the "3D map" and automatic charging by "drone port," which verified that the long-distance autonomous drone flight is technically possible. *www.terra-drone.net*

SunPower to receive automated access for drone flights

SunPower Corp. has announced that it is the first company to receive approval from the U.S. Federal Aviation Agency (FAA) for automatic access to operate a drone in regulated airspace over controlled airports.

The new access category, called Low Altitude Authorization Capability (LAANC), was released recently in a beta test at four airports including San Jose (SJC), Cincinnati International Airport (CVG), Reno (RNO), and Lincoln (LNK). SunPower received LAANC authorization through Skyward, an FAA-approved vendor. *www.sunpower.com*

Dedrone unveils next generation software to counter malicious drones

Dedrone has announced their next generation software upgrade, DroneTracker 3. It is the industry's first airspace security solution that includes automated summary reporting for instant diagnosis of drone airspace activity. It brings significant enhancements for customers including: automated summary reporting, enabling security personnel to instantaneously assess and analyze drone threats, enterprise-grade security

and management, allowing for multi-user management and seamless integration into existing security programs, increased simplification of platform set up, creating an intuitive and quick-to-deploy system

Terra Drone And LG U+ Put UTM System Into Commercial Use

Terra Drone Co., Ltd., has commercialized UTM(Unmanned Traffic Management) system for the first time in Korea collaborating with LG U+, a South Korean cellular carrier owned by LG Corporation.

NOAA, UTSI Test Electric UAV With Autopilot

The Atmospheric Turbulence and Diffusion Division (ATDD) of the National Oceanic and Atmospheric Administration's (NOAA) Air Resources Laboratory is combining Black Swift Technologies' (BST) SwiftCore flight management system (FMS) with UAV Factory's Penguin BE drone in support of a joint research project with the University of Tennessee Space Institute (UTSI).

ATDD, located in Oak Ridge, Tenn., focuses on research on air quality, climate and boundary-layer processes both nationally and globally. Air quality research objectives include improving the understanding of air-surface exchange processes and increasing the predictive capabilities of air quality models.

According to BST, which is based out of Boulder, Colo., this project represents the first integration of its SwiftCore autopilot FMS with UAV Factory's Penguin BE unmanned aerial vehicle (UAV), an electric-propulsion drone with a 3.3-meter wingspan

Alibaba's drones deliver packages to islands

Chinese e-commerce giant Alibaba has announced that it has used UAVs to deliver packages over water for the first time. Three drones carrying a total six boxes of passionfruit with a combined weight of around 12 kilograms flew from Putian in East China's Fujian province to nearby

Meizhou Island on Oct 31. The drones were jointly developed by Alibaba's delivery arm Cainiao Network, the company's rural shopping platform Rural Taobao, and a domestic technology firm. *www.chinadaily.com.cn/*

Pix4D partnership with KKC

To deliver a i-Construction-compliant drone mapping and photogrammetry solution for the Japanese market, Pix4D has partnered with Kokusai Kogyo Corporation (KKC), a Japan-based geospatial consulting company. i-Construction is a set of government-defined regulations to govern the collection and processing of drone data. The partnership will jointly develop the service and new features to meet the requirements for public surveying and i-Construction standards.

FAA Details UAS Integration Pilot Program

The FAA published a notice on the Unmanned Aircraft Systems (UAS) Integration Pilot Program this week. The program, initiated by a Presidential Memorandum, is designed to accelerate safe UAS integration through public-private sector partnerships.

Few highlights are as follows
- Companies must team with local, state or tribal governments to apply.
- Applicants will provide proposals for the creation of "innovation zones," where they can conduct more advanced UAS operations than those typically allowed under current regulations, including beyond line-of-sight flights, operations over people, and operations at night.
- The U.S. Department of Transportation will use data generated from this program to advance the state of the industry by developing enabling regulations to increase drone operations.

Complete details could be accessed at FAA website. *www.faa.gov*

Fujitsu and HERE partnership

Fujitsu and HERE Technologies have announced a plan to link their respective technologies into powerful integrated solutions for customers developing advanced mobility services and autonomous cars. The two companies have signed an agreement with a view to commencing a long-term strategic partnership that would benefit both companies' customers. *www.fujitsu.com*

Navya puts its self-driving shuttle tech in an autonomous taxi

Navya has announced its Autonom Cab vehicle, which is built to haul up to six people around cities without a driver. The Autonom Cab is essentially a smaller, higher-speed version of Navya's self-driving shuttles that have been roaming around the University of Michigan and will start plying Las Vegas' roads soon. While those drive at around 15 miles per hour, the Autonom Cab will zip around city streets at an average of 30 mph, carting people to and from their destinations. And just like the shuttles, the Cab doesn't have a driving wheel or pedals, meaning it's built to be level 4 ADS-DV autonomous and require no human input to move. *www.engadget.com*

17 million wireless IoT devices in agriculture in 2016

According to a research report from Berg Insight, the installed base of wireless IoT devices in agricultural production worldwide reached 17.0 million connections in 2016. The number of wireless connections is forecasted to grow at compound annual growth rate of 10.0 percent to reach 27.4 million in 2021. There is a broad range of wireless technologies used in agricultural production with different characteristics and use cases. 802.15.4-based standards comprise the most employed wireless technology due to its wide adoption in dairy cow monitoring applications. The main application areas for cellular communication are machine telematics and remote monitoring via in-field sensor systems. Cellular connections amounted to 0.8 million at the end of 2016 and is expected to grow at a CAGR of 30.2 percent to reach 3.1 million in 2021.

Microsoft launches Azure LBS for geospatial needs across industries

Azure LBS customers are guaranteed trusted location data through TomTom's unique feedback loop ecosystem – a global community of users continually providing map and traffic data resulting in richer content and more trustworthy data. As part of Azure LBS, customers can now build with a wide array of TomTom API services under the Microsoft Azure brand including Search and Geocoding, Routing, Traffic and Maps.

It also offers many options for customization and opportunities beyond connected cars to power smart cities, IoT and industrial applications in sectors ranging from manufacturing to retail to automotive. ◺

Munich, March 5–7, 2018

Register by Jan 15, 2018 to receive the early rate!

Quelle Illustration: Creativ Market/by Sky Pics Studio and ARTICA, iStockphoto – alle bearbeitet

MUNICH SATELLITE NAVIGATION SUMMIT 2018

www.munich-satellite-navigation-summit.org

Leica ScanStation P50 enables users to scan the inaccessible

Leica Geosystems have released the Leica ScanStation P50, the fastest and safest long-range 3D laser scanner, as the newest member of the 3D terrestrial laser scanner P-Series. It combines all the well-known features of the P40 plus a longer-range scanning capability of more than 1 kilometre. Increasing users' flexibility to offer services in new markets, this rugged and versatile laser scanner enables professionals to 3D capture even at great distances with angular accuracy paired with low range noise and survey-grade dual-axis compensation.

ABB selects Digpro's dpPower

ABB selects dpPower and the GIS software solutions from Digpro to support the migration of network data, and to support the process and work flow for Network Planning and Design of the electrical network including geo-spatial visualization of all network assets in scope, and to feed the ADMS calculation engines with accurate network data.

The project includes implementation and rollout of an integrated system with GIS/NIS, SCADA and ADMS capabilities. The customer operates a large electrical distribution network in Turkey, and provides services to more than 1.7 Million customers. *www.digpro.com*

PPP Module comes to Carlson SurveyGNSS

Carlson SurveyGNSS, Carlson Software is now enhanced by Precise Point Positioning (PPP) as an add-on module. With the new Carlson module, PPP, users can post- process using a single receiver. PPP adds precise GNSS station positioning capabilities for a single GNSS receiver operating autonomously. It is useful for obtaining submeter to centimeter level absolute positioning accuracies.

Carlson Precision 3D Topo 2018

Carlson Software's Precision 3D Topo 2018 featuring enhanced visual photographic background, point cloud loading and editing, polyline best fit alignment, and much more has been released.

New 2018 features include enhanced visual Google Maps photographic background, automated Google surface creation, 3D Model editing, polyline editing tools, additional snap modes, and improved DXF import/export for surfaces, polylines and points. Users are able to import survey data, points, polylines, surfaces, point clouds, both traditional LIDAR and aerial drone survey data, and more from a wide variety of programs and entities to create useable 3D surfaces.

Tersus announces BX316D

Tersus GNSS Inc. Has announced BX316D to extend its GNSS OEM RTK & PPK board, and offer more compatibility to the market. BX316D is a GNSS RTK OEM board for accurate positioning and heading. It is able to integrate with other host devices or to serve as an independent positioning system. The versatile interface and log/command formats make it compatible with major GNSS OEM boards in market. *www.tersus-gnss.com*

Trimble Expands CenterPoint RTX FAST Correction Service

Trimble has announced the expansion of its CenterPoint® RTX Fast (RTX Fast) correction service in North America and Europe. RTX Fast reduces the convergence time—the duration needed to reach full precision accuracy—by up to 98 percent faster than other satellite-delivered correction services. The service allows customers to realize horizontal positioning accuracy of better than 4 centimeters (1.5 inches) in as fast as one minute. No other satellite-delivered correction service on the market today can provide this combined level of accuracy and convergence performance. With RTX Fast, farmers, surveyors, GIS professionals and construction contractors can work faster, improve productivity, minimize input costs and reduce worker fatigue. New RTX Fast services have recently launched in Switzerland, Slovakia, Northern Italy, Eastern Poland and the Southern regions of Saskatchewan and Manitoba. *www.trimble.com/Positioning-Services/RTX.*

Hexagon Safety & Infrastructure Unveils Safe City Framework

Hexagon Safety & Infrastructure unveiled its Safe City Framework recently. It offers flexibility to support solutions that advance capabilities, while being practical to implement within a city's new or existing information and communications technology (ICT) infrastructure. Hexagon has been independently assessed as the global market leader for computer-aided dispatch (CAD) and GIS software in control rooms and offers an extensive portfolio of solutions and domain expertise for other vital public services. *www.hexagon.com*

NovAtel partners with Esterline on aviation GNSS receiver

Esterline CMC Electronics and NovAtel Inc. have entered a new strategic partnership, extending their collaboration in GNSS positioning technology that started in the late 1990s.

The partnership will see NovAtel's GNSS measurement technology integrated into a new Esterline CMC-designed multi-constellation, multi-frequency chipset for certified aviation use. The DO-254 Level A certified chipset will allow both companies to develop new GNSS receiver solutions for use in a variety of safety critical applications, including DO-178C Level A certified products designed for commercial aviation, military and unmanned aerial systems (UAS).

Combining the capabilities of NovAtel's GNSS expertise with Esterline CMC's aviation and certification experience will allow the companies to bring innovative solutions to the market, meeting the requirements of new and evolving industry standards as the modern age of multi-constellation, multi-frequency GNSS positioning in aviation is ushered in, the companies said.

Harris completes navigation payload for GPS III satellites

Harris Corporation has completed development of its fully digital Mission Data Unit (MDU), which is at the heart of its navigation payload for Lockheed Martin's GPS III satellites 11 and beyond.

The current Harris payload for GPS III space vehicles (SVs) 1-10 includes a greater than three times reduction in range error, up to eight times increase in anti-jamming power, added signals — including one compatible with other GNSS — and greater signal integrity.

Harris' GPS III SV11+ fully digital navigation payload will further improve on performance for the U.S. Air Force by providing more powerful signals, plus built-in flexibility to adapt to advances in GPS technology, as well as future changes in mission needs.

East View Geospatial offers Norwegian Nautical Charts

East View Geospatial (EVG) has announced an agreement with Kartverket, the Norwegian Mapping and Cadastre Authority, to offer digital nautical charts of Norwegian waters. This agreement expands upon the existing EVG-Kartverket partnership, allowing EVG to distribute GeoTIFF charts and S57 vector data in addition to EVG's print-on-demand services for Kartverket charts. *www.eastview.com*

Esri Supports the Geospatial Data Act

Esri Inc. have applauded Congress in introducing the Geospatial Data Act (GDA) of 2017 (S. 2128/H.R. 4395). Legislative sponsors Senator Orrin Hatch (R-UT) and Senator Mark Warner (D-VA), U.S. Representative Bruce Westerman (R-AR-04), and U.S. Representative Seth Moulton (D-MA-06) demonstrated remarkable leadership in collaborating with GIS organizations across government and industry to advocate for common data standards, interagency collaboration, and transparency to taxpayers on shared national data services.

"3-D mobile mapping will grow as we meet the needs of our growing population"

says Stuart Woods, Vice President, Geospatial Solutions Division, Leica Geosystems AG in an interview with Coordinates...

How does 3-D capture technologies help to 'understand infrastructures' better?

The world is not flat. By working with 3-D technologies, we are able to represent our world in a model which best approximates reality. This enables us to compare to plans and monitor our world in this model – it enables us to accelerate building new infrastructures by knowing the exact dimensions that we are starting with. It is our best tool today to enable growth.

What challenges did you keep in mind while developing a product like Pegasus:Two?

A tool should not limit how, when, or where a user captures data. We worked hard to make the Pegasus:Two as flexible and vehicle independent – as possible. We wanted to create a product which was fast to deploy while also being flexible in how the user would use this tool. This was our key focus.

How do you see the growth of 3-D technologies in the years to come?

The population is growing fast and people need to be mobile. They are travelling by car, bus and train every day – to work, to school, or to visit friends and family. The safety and security of the transportation network is important while focusing on assuring the capacity is in place to meet the growing demand of travel. The only way to meet these demands is to increase the efficient and effectiveness of infrastructure construction – while using the same tools to monitor the infrastructure for safety and security. 3-D mobile mapping and mobile solutions will grow as we meet the needs of our growing population.

What are the future innovations you foresee in 3-D survey and mapping domain?

Future innovations from Leica Geosystems in 3D and mapping will continue our original goals – not limiting how, when, or where a user captures. We have already showed with the Pegasus:Backpack that a user can capture indoors – this will expand. Leica Geosystems is leading the marketing in making the hardware independent of how, where, and when a capture is done!

How cost effective is to use a mobile mapping technology?

Mobile mapping currently provides the most cost-effective solution to 3-D capture. A single capture enables the user to use the data multiple times while also accelerating the time to engineering drawings. Using Mobile Mapping makes sure there are no site revisits since the site is brought back to office in the form of point clouds.

One of the reasons for NHAI (National Highway Authority of India) to mandate the use of Mobile Mapping for Road Survey was to mitigate the delay caused due to human error and also how conventional methods missed important infrastructure from site. With India moving the Smart City way Time is money and Mobile Mapping is how we save Time and Cost over runs due to repeated site visits in the form of Survey Crew and their Logistic expense on site.

Agreeing to a common vision will make it easier for federal, state, and local agencies to integrate location data into widespread practice, no matter their size. The American Association of Geographers' (AAG) industry leadership brought the GIS community together to shape this bipartisan legislation that works for all organizations.

Hemisphere GNSS enhanced Atlas system

Hemisphere GNSS has announced a series of major enhancements to its Atlas GNSS Global Correction Service, including Atlas Basic, Atlas AutoSeed, and the addition of global ionospheric modeling to the system. Atlas is a flexible, scalable, and industry-leading GNSS-based global L- band correction service, providing robust performance and correction data for GPS, GLONASS, and BeiDou, at market-leading prices. Delivering its correction signals via L-band satellites at accuracies ranging from meter to sub-decimeter levels, Atlas also leverages approximately 200 reference stations worldwide, providing coverage to virtually the entire globe. *www.HGNSS.com*

Autodesk and Esri Partnership

Autodesk, Inc. and Esri, Inc. have announced the start of a new relationship to build a bridge between BIM and GIS mapping technologies. Together they plan to enable a broad range of industries to gain better context by visualizing data of the man-made world, the environment, citizens and the networks that weave it all together.

For infrastructure owners around the world, both public and private, enabling BIM and GIS mapping software to more seamlessly work together will optimize their ability to plan, design, build and operate infrastructure assets saving precious time and money. Improving the integration of Esri and Autodesk software has the potential to dramatically decrease workflow times. *www.esri.com*

MARK YOUR CALENDAR

January 2018

14th International Conference on LBS
15 - 17 January
Zurich, Switzerland
http://lbs18.ethz.ch

February 2018

18th Annual International LiDAR Mapping Forum
5 - 7 February
Denver, USA
www.lidarmap.org

GMA: Geodesy, Mine Survey and Aerial Topography
15 – 16 February
Moscow Novotel Center, Russia
http://www.con-fig.com/?lang=eng

March 2018

Munich Satellite Navigation Summit
5 - 7 March
Munich Germany
www.munich-satellite-navigation-summit.org

EUROGEO 2018
15 - 17 March
Cologne, Germany
www.eurogeography.eu

Gi4DM 2018
18 - 21 March
Istanbul Technical University, Turkey
gi4dm2018.org

April 2018

The 7th Digital Earth Summit 2018
17 – 19 April
El Jadida, Morocco
http://www.desummit2018.org/

9th IGRSM International Conference and Exhibition on Geospatial & Remote Sensing (IGRSM 2018
24-25 April 2018
Kuala Lumpur, Malaysia
https://igrsmconf18.wixsite.com/igrsm2018

International Navigation Forum Navitech 2018
24-27 April
Moscow, Russia
www.glonass-forum.ru

May 2018

Geoscience-2018
2-4 May
Rome, Italy
http://geoscience.madridge.com/index.php

12th Annual Baška GNSS Conference
6 - 9 May
Baška, Croatia
www.rin.org.uk

FIG Congress 2018
6 - 11 May
Istanbul, Turkey
www.fig.net/fig2018/

The European Navigation Conference 2018
14 - 17 May
Gothenburg, Sweden
www.enc2018.eu

GEO Business 2018
22 - 23 May
London, UK
http://geobusinessshow.com

June 2018

HxGN LIVE 2018
12-15 June
as Vegas, USA
http://hxgnlive.com

7th International Conference on Cartography & GIS
18-23 June
Sozopol, Bulgaria
www.iccgis2018.cartography-gis.com

July 2018

GI Forum 2018
3 - 6 July
Salzburg, Austria
www.gi-forum.org

Esri International User Conference 2018
9 - 13 July
San Diego, USA
www.esri.com/events

September 2018

Inter Drone 2018
5 - 7 September
Las Vegas, USA
www.interdrone.com

ION GNSS+ 2018
24 - 28 September
Miami, USA
www.ion.org

October 2018

Joint Geo Delft Conference
The 6th International FIG 3D Cadastre Workshop
The 3D GeoInfo Conference
1- 5 October
Delft, the Netherlands
www.tudelft.nl/geodelft2018

Intergeo 2018
17 - 18 October
Frankfurt, Germany
www.intergeo.de

December 2018

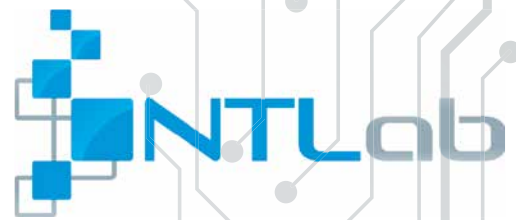**The 16th IAIN World Congress 2018**
28 November - 1 December
Chiba, Japan
https://iain2018.org
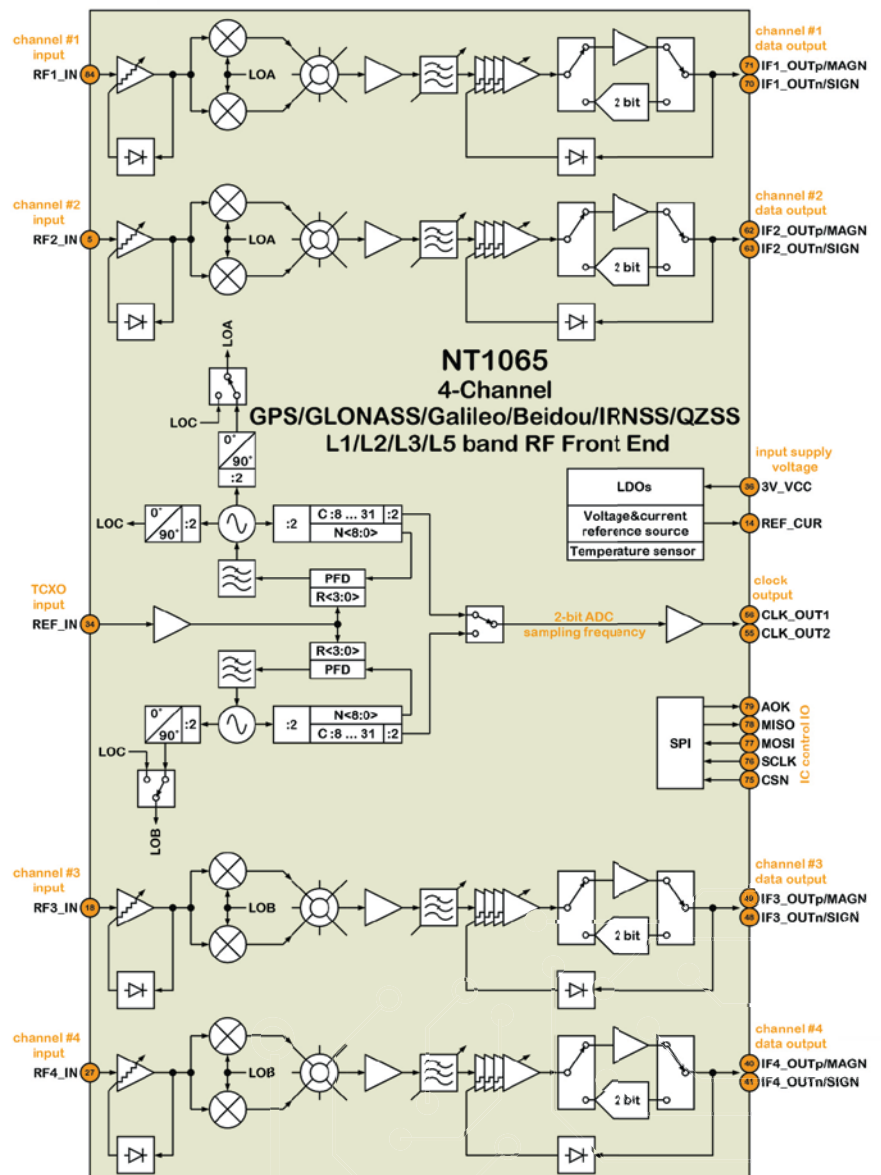
NT1065

4-channel GNSS RFFE IC

Precision is going to be
simpler, cheaper, faster ...

NT1065 is a 4-channel GNSS RF Front-End chip for professional navigation market: geodesy, driverless cars, drones and similar applications.

The feature list includes:

- simultaneous reception of GPS/GLONASS/Galileo/BeiDou/IRNSS/QZSS signals

- frequency bands: L1/L2/L3/L5/E1/E5a/E5b/E6/B1-C/B1I(Q)/B1-2I(Q)/B2/B3

- full programmability of each of 4 channels (signal bandwidth, downconversion sideband, AGC options, analog/2-bit digitized output, etc.)

- simple and easy-to-use register map for chip configuration.

NT1065 also could be used by GNSS researchers to create sophisticated front-ends for their receivers.
For such purposes, we offer wide selection of evaluation kits: with 4 and more channels, analog and digitized outputs, connectable to PC or FPGA platforms.

NT1065
4-Channel
GPS/GLONASS/Galileo/Beidou/IRNSS/QZSS
L1/L2/L3/L5 band RF Front End

www.ntlab.com   info@ntlab.com

NT1065 is already in mass production. Fabricated by amsAG, Austria. ams